

Review

# Synthetic and Structural Chemistry of Uranyl-Amidoxime Complexes: Technological Implications †

Sokratis T. Tsantis <sup>1,\*</sup> , Maria Iliopoulou <sup>1</sup>, Demetrios I. Tzimopoulos <sup>2</sup> and Spyros P. Perlepes <sup>1,\*</sup><sup>1</sup> Department of Chemistry, University of Patras, 26504 Patras, Greece; marion.hliop@gmail.com<sup>2</sup> Department of Chemistry, Aristotle University of Thessaloniki, 54124 Thessaloniki, Greece; dimtzim@auth.gr

\* Correspondence: sokratis.t.tsantis@gmail.com (S.T.T.); perlepes@upatras.gr (S.P.P.)

† Dedicated to the loving memory of Konstantin A. Tsipis, a great theoretical chemistry scientist, a fantastic mentor and a precious friend.

**Abstract:** Resource shortage is a major problem in our world. Nuclear energy is a green energy and because of this and its high energy density, it has been attracting more and more attention during the last few decades. Uranium is a valuable nuclear fuel used in the majority of nuclear power plants. More than one thousand times more uranium exists in the oceans, at very low concentrations, than is present in terrestrial ores. As the demand for nuclear power generation increases year-on-year, access to this reserve is of paramount importance for energy security. Water-insoluble polymeric materials functionalized with the amidoxime group are a technically feasible platform for extracting uranium, in the form of  $\{UO_2\}^{2+}$ , from seawater, which also contains various concentrations of other competing metal ions, including vanadium (V). An in-depth understanding of the coordination modes and binding strength of the amidoxime group with uranyl and other competing ions is a key parameter for improving extraction efficiency and selectivity. Very limited information on the complexation of  $\{UO_2\}^{2+}$  with amidoximes was available before 2012. However, significant advances have been made during the last decade. This report reviews the solid-state coordination chemistry of the amidoxime group (alone or within ligands with other potential donor sites) with the uranyl ion, while sporadic attention on solution and theoretical studies is also given. Comparative studies with vanadium complexation are also briefly described. Eight different coordination modes of the neutral and singly deprotonated amidoxime groups have been identified in the structures of the uranyl complexes. Particular emphasis is given to describing the reactivity of the open-chain glutardiamidoxime, closed-ring glutarimidedioxime and closed-ring glutarimidoxioxime moieties, which are present as side chains on the sorbents, towards the uranyl moiety. The technological implications of some of the observed coordination modes are outlined. It is believed that X-ray crystallography of small uranyl-amidoxime molecules may help to build an understanding of the interactions of seawater uranyl with amidoxime-functionalized polymers and improve their recovery capacity and selectivity, leading to more efficient extractants. The challenges for scientists working on the structural elucidation of uranyl coordination complexes are also outlined. The review contains six sections and 95 references.

**Keywords:** recovery of uranium from seawater; amidoxime-functionalized synthetic polymers; structural chemistry of uranyl-amidoxime model complexes; coordination chemistry



**Citation:** Tsantis, S.T.; Iliopoulou, M.; Tzimopoulos, D.I.; Perlepes, S.P. Synthetic and Structural Chemistry of Uranyl-Amidoxime Complexes: Technological Implications. *Chemistry* **2023**, *5*, 1419–1453. <https://doi.org/10.3390/chemistry5020097>

Academic Editor: Catherine Housecroft

Received: 1 April 2023

Revised: 18 May 2023

Accepted: 31 May 2023

Published: 13 June 2023



**Copyright:** © 2023 by the authors. Licensee MDPI, Basel, Switzerland. This article is an open access article distributed under the terms and conditions of the Creative Commons Attribution (CC BY) license (<https://creativecommons.org/licenses/by/4.0/>).

## 1. Introduction—Scope and Organization of This Review

Intensive research over the last two decades has been devoted separately to the chemistry of 5f metals or actinoids (An), especially that of U [1], and the coordination chemistry of amidoximes [2]. An amalgamation of these two areas emerged after 2010. This was due to the fact that insoluble polymer substrates, functionalized with the amidoxime group ( $R-C(NH_2)=NOH$ ; AO), were demonstrated to be a useful technical platform for extracting uranium, in the form of  $\{U^{VI}O_2\}^{2+}$ , from seawater [3–9], a potential source

of extremely abundant U, for use as nuclear fuel. In the most recent reference [9], the authors provide guidance for rationally designing and synthesizing new, amidoxime-based adsorbents, and give suggestions for solving the technical problems related to uranium extraction from seawater and uranium removal from effluents in the near future. This area of study is old (*vide infra*), but the intense interest of inorganic chemists in this field is new. Many of them have been trying to understand how the uranyl ( $\{U^{VI}O_2\}^{2+}$ ) ion (but also other metal ions present in seawater) binds to uranium-selective amidoxime-functionalized sorbents by experimentally determining the solid-state structures of uranyl complexes with molecules simulating the possible binding sites and characterizing these sites spectroscopically. Spectroscopy can provide scientists with spectral features which can be used to identify the actual adsorbed species on uranium-loaded sorbents. The overall goal is to optimize the selectivity of AO extractants for uranyl over other metal ions of seawater, an issue that is likely exacerbated by the enigmatic binding modes to  $\{U^{VI}O_2\}^{2+}$ . This review comprehensively covers the structural chemistry of uranyl complexes with ligands containing one or more amidoxime groups. The term “structural chemistry” refers to the metal complexes with molecular (and crystal) structures that are known through single-crystal X-ray crystallography. The technological implications of the structures, with respect to the selective extraction of uranium from seawater using amidoxime-based sorbents, will be outlined. Solution [10–12] and theoretical [13–17] reports on this general topic are very limited. Thus, apologies are due to the researchers whose excellent work will not be mentioned here. This review is a consequence of our research efforts in the chemistry of actinoids [18–22], with emphasis on the use of oxime- and AO-based ligands [23–25]; the latter area contains a plethora of unpublished work from our group, which will be briefly described.

The content of the review is chemical, and it is assumed that the reader has a fundamental knowledge of coordination chemistry. To avoid long synthetic descriptions, balanced chemical equations will be used; these are written using molecular—and not ionic—formulae. In the synthetic part of this review, the philosophy behind the reaction schemes and the choice of the AO ligands will be explained. The method that will be used to describe the coordination of ligands to metal ions herein is the widely accepted “Harris Notation” [26]. This method describes the coordination mode as  $X.Y_1Y_2Y_3 \dots Y_n$ , where  $X$  is the number of metal ions bound by the ligand, and each  $Y$  value refers to the number of metal sites attached to the different metal ions. The order of the  $Y$  groups follows the Cahn–Ingold–Prelog priority rules; thus, for the ligands reported in this work, O is placed before N. In cases where one (or more) donor atom, e.g., N, is coordinated, while another (or other) donor atom of a similar type, e.g., N, is “free” (i.e., not coordinated), then we first assign an integer number (1, 2, ...) to the coordinated donor atom(s) in decreasing order, and then we use nil for the “free” one(s). If the nitrogen atom cannot form a coordination bond because of its protonation, we do not give a number in the notation. For clarity purposes, the coordination modes of the AO ligands will be presented schematically.

This is the first attempt to summarize and discuss critically the structural chemistry of uranyl–amidoxime complexes. The topic has been *partly* and *briefly* covered in an excellent and seminal review [27].

This work is organized as follows: Sections 2 and 3 describe, in a short way, the current interest in the U (and especially uranyl) chemistry and the coordination chemistry of the amidoxime group, respectively. Section 4 is a brief history of the attempts to recover of seawater U; it gives a summary of the materials for the recovery of U from seawater, with an emphasis on AO-containing synthetic polymers. Sections 2–4 are an “hors d’oeuvre” of the review. Section 5 is the “main menu” of this scientific “meal”, giving details for the synthesis and structures of the uranyl complexes; the discussion is arranged in parts according to the ligand. At the end of each part, some concluding comments in terms of the technological implications of the results will be provided. The last section (Section 6) will summarize the main points of the topic under discussion and illustrate perspectives and ideas for further work.

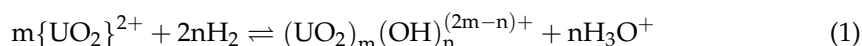
## 2. The Current Interest in Uranium Chemistry and the Renaissance of the Uranyl Complexes

Uranium was first isolated from pitchblende in 1789 by Klaproth, and it owes its name to the planet Uranus. This planet had been discovered 8 years earlier by the astronomer Herschel. There are two milestones in the history of U. The first was in 1895, when Becquerel provided strong evidence that this element undergoes radioactive decay. The second was in 1938, when it was discovered that  $^{235}\text{U}$  undergoes fission with slow neutrons, creating chain reactions which led to the production of weapons (the Manhattan Project). It was the first f element that was isolated, and caused confusion during the first decades of the development of the Periodic Table. At the beginning, it was classified as transition metal due to its similarity with the Group 6 metals, until Seaborg understood the existence of the 5f series. U is often considered as having “Dr. Jekyll and Mr. Hyde” behavior. There are two reasons for this. From the chemical viewpoint, U sometimes behaves like lanthanoids, but at other times (and more often) it acts as a transition metal [1]. The second reason refers to its applications. It can be used for the construction of destructive nuclear weapons, but also as a nuclear fuel for peaceful purposes.

The description of the inorganic chemistry of U is outside the scope of this review. The interested reader can find information in standard inorganic chemistry textbooks and in our recent review [18].

The inorganic chemistry of this element currently attracts the intense interest of many groups around the world for a variety of reasons [1,28–42]. Some topics of research, among others, are the development of non-aqueous uranium chemistry [1,29], the identification of unusual oxidation states of the element in molecular compounds [30], the investigation of their magnetic properties [1,40–42], the study of the chemistry of uranium–nitrogen multiple bonds [33,39], the proposal of new reagents for the reduction of the levels of radioactivity in waste nuclear fuels, the finding of methods to accomplish multi-electron reactions related to organometallic transformations and to improve the U potential in small-molecule activation [36] and advanced theoretical studies [35,37]. A recent example of a compound with U at the oxidation state +I is the synthesis of a salt of  $[\text{U}^{\text{I}}(\eta^5\text{-C}_5^i\text{Pr})_2]^-$  ( $^i\text{Pr}$  is the isopropyl group) isolated from the corresponding U(II) metallocene by reduction with potassium graphite [30]. The great activity of U chemistry is evidenced by the fact that nearly 60% of all entries for this metal in the Cambridge Structural Database have been deposited within the last 15 years.

The linear *trans*-dioxouranium(VI) (uranyl) cation, *trans*- $[\text{U}^{\text{VI}}\text{O}_2]^{2+}$ , is the most common, stable, abundant and prevalent species of uranium(VI) in aqueous solution and in the environment [17]; exceptions are a few molecular compounds, such as  $\text{UOF}_4$ ,  $\text{UF}_6$  and  $\text{UCl}_6$ , and some alkoxides, such as  $\text{U}(\text{OMe})_6$ . Uranyl compounds eventually result from the exposure of compounds of U in lower oxidation states to air. The uranyl cation has been used in colorings since Roman times, and displays a green fluorescence (a result of a ligand-to-metal charge transfer) in the solid state and in solution. This fluorescence was noticed by Brewster in 1843, and later led to the discovery of the Stokes shift and radioactivity. The uranium–oxygen bond of the uranyl cation is formally triple, the two  $\pi$  bonds being formed by  $6d_{xz}-2p_x$  and  $5f_{xz^2}-2p_x$  overlaps, while the  $\sigma$  bond is formed though the overlap of O(2p)  $\sigma$  orbitals with a  $\text{U}^{\text{VI}} 6d_z^2$  orbital and a hybrid orbital derived by mixing  $5f_z^3$  with  $6p_z$ . The equatorial coordination sites in the uranyl ion are usually occupied by 4–6 ligand donor atoms in its complexes, resulting in square, pentagonal (most common) and hexagonal bipyramidal environments. In the reactivity studies, the two oxo groups are usually inert. Formation of oligomeric or polymeric species takes place in an aqueous solution, Equation (1). The oligomerization process proceeds through the sharing of hydroxo or oxo (from  $\text{H}_2\text{O}$ ) groups. This hydrolysis is promoted at pH values > 4 and depends on the uranyl concentration.



The  $\{UO_2\}^{2+}$  dominates the chemistry of U. There has been an explosive growth of interest in this ion, mainly in the last 15 years, for many reasons, including: (i) the chemical, thermal and photochemical functionalization of the oxo groups of this cation [43,44]; (ii) the synthesis of anionic uranyl complexes with large pores for successful removal of the radiotoxic  $^{127}Cs^+$  ions [45]; (iii) aspects of metallosupramolecular chemistry, for example the behavior of neutral uranyl complexes with polydentate chelating Schiff-base ligands to act as anion receptors [46]; (iv) the efficient uptake of  $\{UO_2\}^{2+}$  by artificial and natural proteins [47]; (v) the chemistry of uranyl complexes with peroxide as ligand [48]; (vi) theoretical aspects [49,50]; (vii) the study of the reactions between the uranyl ion and polycarboxylate ligands [51]; (viii) the employment of  $\{UO_2\}^{2+}$  as a templating agent for the synthesis of macrocyclic complexes [52]; (ix) the efficiency of uranyl complexes to act as selective homogeneous catalysts [53]; (x) the use of uranyl complexes in separation processes associated with nuclear fuel processing and nuclear waste management [54,55]; (xi) the synthesis of heterometallic  $\{UO_2\}^{2+}$ -3d [54] and  $\{UO_2\}^{2+}$ -4f [56] complexes which have properties of hybrid materials; and (xii) the unique photocatalytic activity, i.e., light-driven (UV or Vis) catalysis, of some uranyl complexes towards several dyes, e.g., methylene blue [57]. As an example of the above areas, the  $UO_2(NO_3)_2 \cdot 6H_2O/H_4Ppb/H_2O_2/KOH$  “blend” in  $H_2O$  gives the giant anionic clusters (obtained as  $K^+$  salts)  $[(UO_2)_{20}(O_2)_{20}(Ppb)_{10}]^{40-}$ ,  $[(UO_2)_{26}(O_2)_{33}(Ppb)_6]^{38-}$  and  $[(UO_2)_{20}(O_2)_{24}(Ppb)_6]^{32-}$ , where  $H_4Ppb$  is benzene-1,2-diphosphonic acid [48]. The  $(UO_2)_{20}$  clusters adopt the fullerene topology, while the  $(UO_2)_{26}$  cluster consists of two building units, related through a  $C_2$  axis, that are connected through organic ligands to form a closed cage. The first cluster is soluble in DMSO, while the second one does not dissolve in this solvent, but it is more soluble in  $H_2O$ , due to the lower proportion of  $Ppb^{4-}$  ligands in the structure. Of significant interest is the study of uranyl–amidoxime interactions which are related to the recovery of uranium from seawater (*vide infra*); these interactions, which are the theme of this review, will be detailed in Section 5.

### 3. Amidoximes: A Class of Interesting Organic Compounds and Exciting Ligands

Amidoximes (Figure 1) are derivatives of primary amides and have the general formula  $R-C(NH_2)=NOH$  (R various, e.g., alkyl and aryl groups). The presence of the  $-NH_2$  group results in a substantial mesomeric effect in several instances, and this creates a significant difference in the chemistry of amidoximes, and that of oximes. The amidoxime functional group is important in pharmaceutical, organic, coordination and material chemistry [58]. The oxime N is basic, whereas the  $-OH$  group is acidic. The  $-NH_2$  group can sometimes be acidic, but only in the presence of metal ions [59]. The acid–base chemistry of amidoximes is illustrated in Figure 2. The most common synthetic route to amidoximes is the reaction of nitriles with  $H_2NOH$  in the presence of  $Na_2CO_3$  or  $NaOH$  in alcohols under reflux (Figure 1); the yields are high (70–90%) [2].



**Figure 1.** The relationship between primary amides and amidoximes (left) and the typical route for the synthesis of amidoximes (right). The term “amidoxime” is frequently used for compounds with the  $-NR_2$  group (R = alkyl, aryl, etc.), but, in this review, the name is confined to molecules possessing the  $-NH_2$  group.

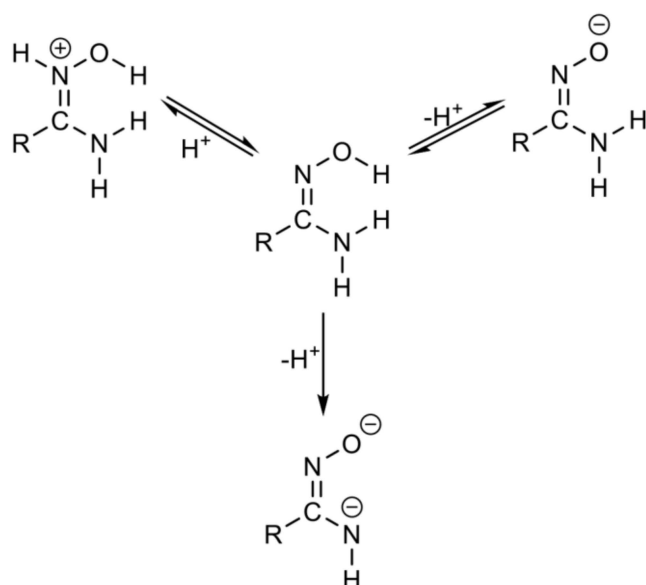


**Figure 2.** Acid–base chemistry of amidoximes.

An important feature of the chemistry of amidoximes is their tautomerism [60,61]. The three major forms are the amidoxime, the aminonitrone and the iminohydroxylamine tautomers (Figure 3). An additional tautomeric form, the *gem*-amino nitroso species, has been suggested, but never experimentally confirmed.

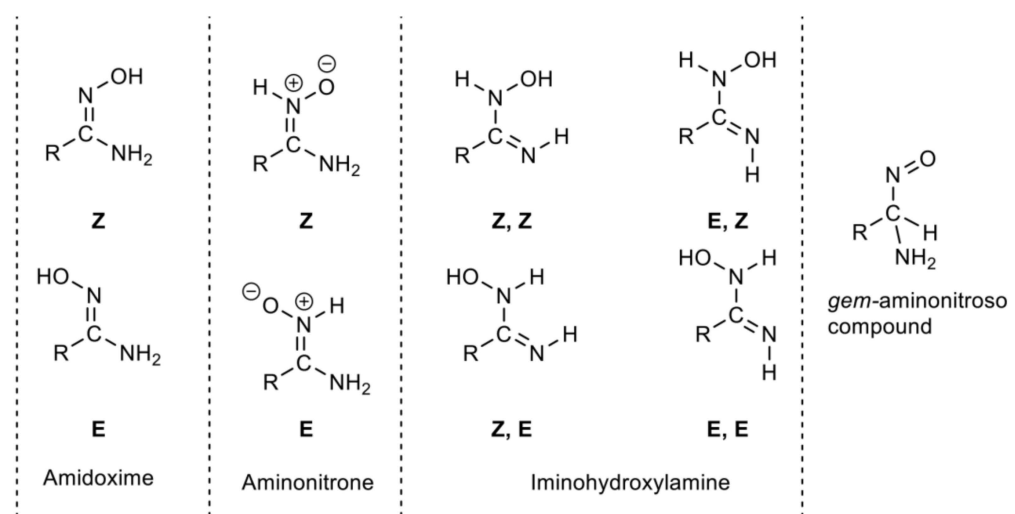


**Figure 3.** The various tautomeric forms of neutral amidoximes.

The IR spectroscopic signatures of  $R-C(NH_2)=NOH$  are the bands at 1680–1650, 950–920 and 3600–3450  $cm^{-1}$ , assigned to the  $\nu(C=N)$ ,  $\nu(N-O)$  and  $\nu(O-H)$  modes, respectively. Most NMR spectra of amidoximes have been recorded in  $d_6$ -DMSO. Two broad singlets at  $\delta$  9.80–8.70 and 6.10–5.20 ppm are assigned to the  $-OH$  and  $-NH_2$  protons, respectively. In the  $^{13}C\{^1H\}$  NMR spectra, the carbon resonance appears at  $\delta$  164–148 ppm, depending on R.

The coordination chemistry of the amidoxime group was partly reviewed 7 years ago [2]. Amidoximes and their deprotonated ( $-1$ ,  $-2$ ) forms possess three centers with a nucleophilic character, i.e., one O and two N atoms. The N atom of the  $-NH_2$  group is  $sp^2$  hybridized and it thus has a very weak basicity. This means that the neutral amino group remains uncoordinated; it forms coordination bonds only when it is deprotonated ( $-NH^-$ ). This is supported by DFT calculations [2], which show that the coordination of the

latter is by  $\sim 18$  kcal/mole more favorable than the former. The to-date crystallographically observed coordination modes of the neutral, singly, and doubly deprotonated forms of the amidoxime group are illustrated in Figure 4. The  $\mu_3$  and  $\mu_4$  modes are extremely rare [2,59].

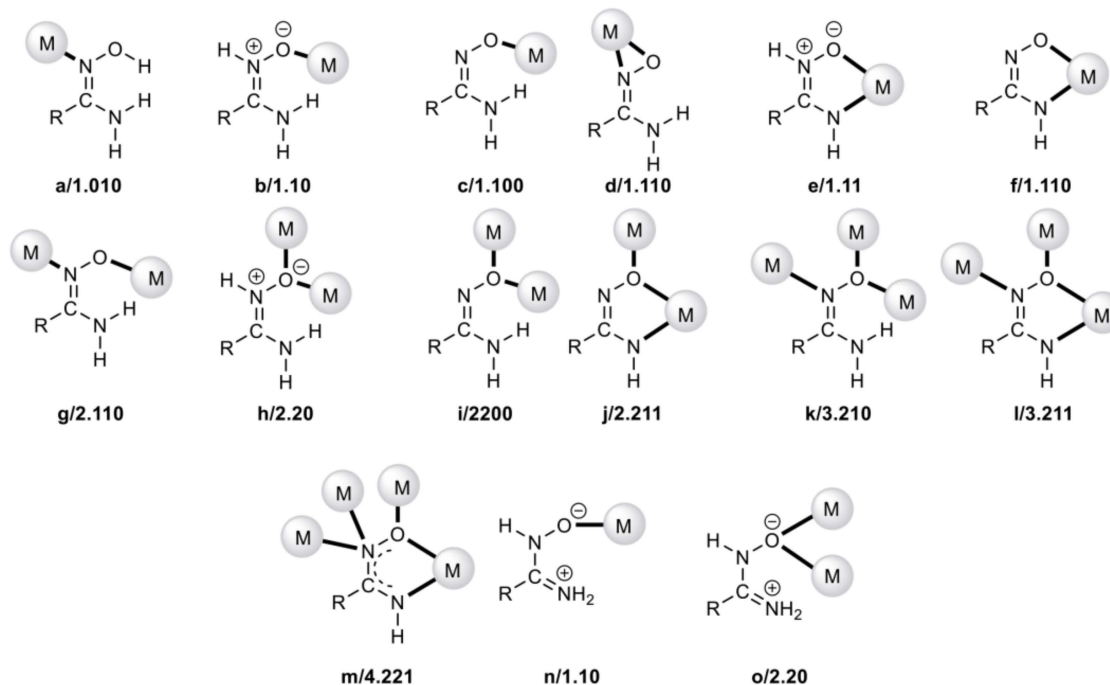


**Figure 4.** The to-date crystallographically established coordination modes of the neutral (**a,b,h,n,o**) amidoxime group, and the monoanionic (**c–e,g,i,k**) and dianionic (**f,j,l,m**) amidoximate groups with any metal. The description of the modes is given using the Harris notation. The negative and positive charges have been drawn only on the neutral amidoxime group to indicate tautomerism. In this scheme, it is assumed that R is a non-donor group; if it has donor atoms, the coordination modes of the resulting ligands are different (and may be more complicated). The coordination bonds are indicated with bold lines.

Of particular interest are [2]: (i) the metal ion-mediated reactions of uncomplexed amidoximes, e.g., the O-iminoacylation of amidoximes via their nucleophilic addition to nitrile ligands, the generation of amidines via nucleophilic oxygenation of CO ligands, the Buchwald–Hartwig N-arylation involving amidoxime species and metal-involving reactions of amidoxime compounds resulting in 5-, 6- or 7-membered heterocycles; (ii) the reactivity of coordinated amidoxime ligands, e.g., nucleophilic addition of amidoximes to nitriles, rearrangement of amidoximes to amidrazones and cyclometallation of amidoximes; and (iii) redox reactions (reduction, oxidation) of amidoximes. A redox reaction from our group is one example of metal-involving reaction of amidoximes [62]. The  $\text{MnF}_2/(\text{py})\text{C}(\text{NH}_2)\text{NOH}/\text{LiOH}$  (1:2:2) reaction system in MeCN/DMSO at room temperature gave complex  $[\text{Mn}^{\text{III}}(\text{bptzpd})_3]$  (**I**), where  $(\text{py})\text{C}(\text{NH}_2)\text{NOH}$  is pyridine-2-amidoxime and  $\text{bptzpd}^-$  is the monoanion of 2,4-bis(2-pyridyl)-1,3,5-triazapentanediene (Figure 5). The  $\text{Mn}^{\text{III}}$  ion is high-spin, “EPR silent” at X-band and the donor atoms of the bidentate chelating ligand are the atoms of the 1 and 5 positions of the triazapentanedienate backbone. It is possible that the reaction proceeds via reduction of the amidoxime group to the corresponding amidine, which undergoes manganese-mediated self-condensation, resulting in the coordinated  $\text{bptzpd}^-$  anion.

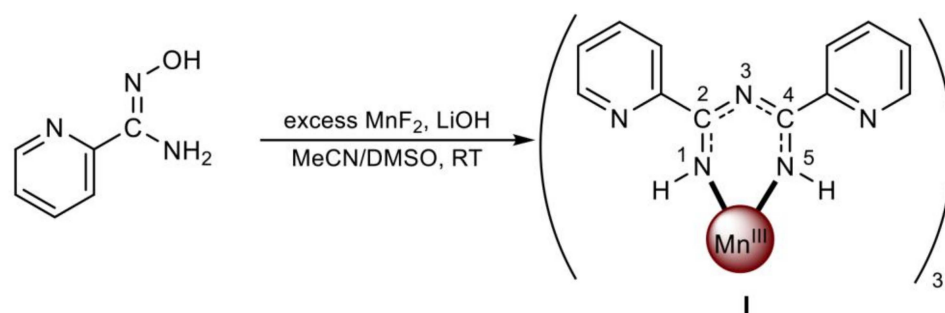


**Figure 5.** Formation of the high-spin complex  $[\text{Mn}^{\text{III}}(\text{bptzpd})_3]$  (I).

#### 4. Extraction of Uranium from Seawater—The Importance of the Amidoxime Sorbents

The International Atomic Energy Agency has predicted that nuclear power production will increase by ~50% over the period 2015–2030 [63–65]. This is expected to result in the depletion of the conventional U reserves until ~2100. Most scientists have not thought in detail about the composition of seawater, and it is probably a surprise for them that the oceans contain uranium. More surprising is the fact that oceans hold a tremendous quantity of this heavy metal. It is believed that more than four (4) billion metric tons of uranium are dissolved in the Earth's oceans. That quantity is estimated to be approximately 1000 times higher than all known terrestrial sources, enough to fuel the nuclear power industry of the world for centuries, even if the demand for uranium grows significantly. The recovery of U from seawater requires a long-term, large-scale and financially viable process of extracting an extremely dilute supply of the metal under difficult and challenging marine conditions. A number of scientific groups have been trying to develop selective and durable adsorbents which can be dropped into the seawater to soak up uranium, withdrawn periodically, stripped of the metal and reused. The researchers are evaluating several types of materials and analyzing the economics of the whole process [27].

The idea of capturing U from the oceans is not new. Researchers at the United Kingdom Atomic Energy Authority worked on this project and published a *Nature* paper in 1964 [66], which describes work published as early as 1953. It was self-evident to scientists 60 years ago, as it is nowadays, that to exploit the ocean's reserves of uranium, an insoluble, high-performance extractant is needed which can work effectively and selectively at the slightly basic pH and high ionic strength of seawater.

U in seawater is in the form of the stable complex  $[\text{UO}_2(\text{CO}_3)_3]^{4-}$  associated with two  $\text{Ca}^{2+}$  ions. The challenge is to discover functional groups, i.e., ligands, that can remove  $\{\text{UO}_2\}^{2+}$  ions from the tricarbonato complex at the seawater concentrations which are 3.3 ppb for uranium and 140 ppm for  $\text{HCO}_3^-$ , and in the presence of other competing ions, such as  $\{\text{V}^{\text{IV}}\text{O}\}^{2+}$ ,  $\{\text{V}^{\text{V}}\text{O}_2\}^+$ ,  $\text{Cu}^{2+}$ ,  $\text{Ca}^{2+}$  and  $\text{Mg}^{2+}$ .

In the last 45 years, three classes of materials have been tested [27,64,65,67–74]. These are inorganic adsorbents (layered metal sulfides or polysulfide-intercalated hydroxides, metal oxides and phosphates, chalcogen sorbents and magnetic adsorbents), nanostructured materials (porous carbon, Atom-Transfer Radical Polymerization for Advanced Adsorbents, Metal-Organic Frameworks, Covalent Organic Frameworks, porous silica and high-affinity genetically-engineered proteins) and synthetic organic polymers (*vide infra*). There are several disadvantages with the former two classes of materials, including solvent losses sustained in solvent extraction methods and the high cost of pumping seawater through columns of inorganic sorbents.

An important period was the early 1980s, when researchers at the Nuclear Research Center in Jülich, Germany, conducted a detailed evaluation of ~200 ion-exchange resin materials. From the materials tested, only poly(acrylamidoximes) met the requirements for chemical stability and selectivity for uranium uptake under real marine conditions. This discovery had as a result the intense focus on such materials in the last 20 years or so. A simplified scheme of the process is illustrated in Figure 6 [11]. Polyethylene or polypropylene fibers are copolymerized with polyacrylonitrile sidechains by a radiation-

induced grafting procedure. Nitrile groups are then converted to amidoxime derivatives by reacting with  $\text{H}_2\text{NOH}$  in  $\text{EtOH}/\text{H}_2\text{O}$  solution. Depending on the reaction conditions (the most crucial parameters are the  $\text{H}_2\text{NOH}$  to nitrile molar ratio and the reaction temperature), a few different amidoxime derivatives can be obtained. The dominant ones are the closed-ring glutarimidedioxime moiety (b, left); the open-chain diamidoxime functionality (a); and the closed-ring glutarimidoxime group (b, right). These moieties can have very different binding abilities with the  $\{\text{UO}_2\}^{2+}$  ion, affecting the overall sorption ability and selectivity of the sorbent material. An impressive progress was made in the late 1990s and early 2000s by Japanese workers, who demonstrated the recovery of more than 1 kg of uranium from ocean currents (several miles from Japan's coastline) in a period of 240 days. They prepared nonwoven sheets of an amidoxime-functionalized polymer and loaded stacks of the sheets, separated by spacer nets, into three large connected cages that were lowered from a floating rig into the Pacific ocean. The USA Department of Energy established a giant research program in 2011, with the central goal being the evaluation and optimization of this technology [65]. The program was successful and increased the adsorbent uranium capacity from 1.5 g to over 6 g of U per kg of the adsorbent material in a period of 30 days. In summary, the basic strategy has two steps: design highly active and selective uranium chelating agents based on the amidoxime functional group and append the ligands comprising those molecular units to a polymeric core in a way that enhances the uranyl binding sites. The implementation of this strategy requires coordination chemistry approaches, among others.

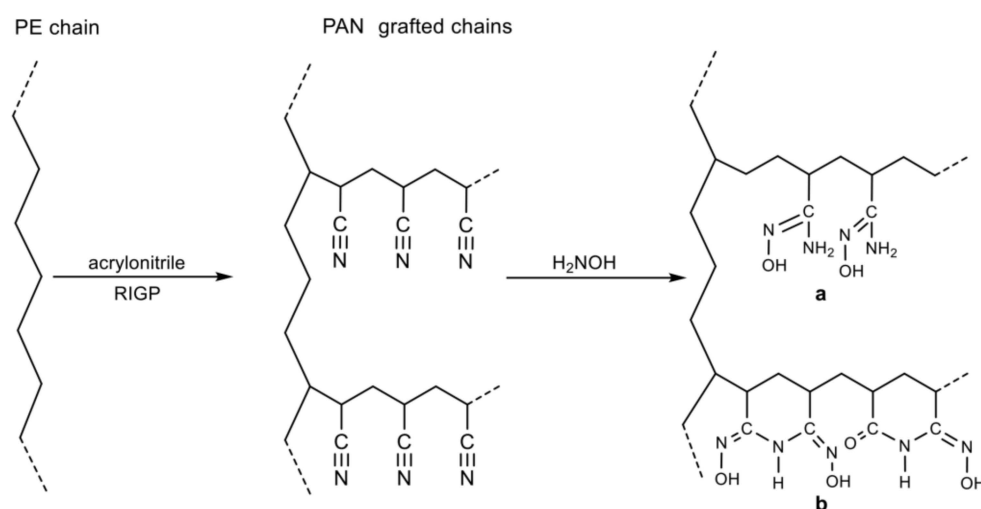


**Figure 6.** Formation of polyacrylonitrile (PAN) side chains and functionalization of PAN to give amidoxime moieties. This scheme is simplified and has been adopted from reference [10]. PE is polyethylene; RIGP is Radiation-Induced Graft Polymerization. (a): Open-chain diamidoxime functionality; (b), left): closed-ring glutarimidedioxime moiety; (b), right): closed-ring glutarimidoxime moiety.

After many years of research several challenges still remain [27]. Several questions remain unanswered, such as: (a) among the possible ligand configurations, formed in the grafting/reaction process, which one has the superior ability toward  $\{\text{UO}_2\}^{2+}$ ? (b) How strongly do the major metal ions (present in seawater) compete with the uranyl ion for sorption and how the selectivity of the sorbent materials can be improved? (c) What are the coordination modes of the ligands when coordinated to uranium or other competing ions that are present in seawater? (d) What is the rate of uranium accumulation under real marine conditions? (e) How can the reusability of the amidoxime-functionalized polymers be improved? Simple coordination chemistry may help with the answers to some of the above questions. It is a paradox that scientists have not still understood why the amidoxime functional group binds  $\{\text{UO}_2\}^{2+}$  so strongly. Even the exact nature of the uranyl-amidoxime

binding mode is ambiguous, and various groups have proposed different possibilities. If we understand the relationship between the amidoxime functionality structure on the polymeric sorbents and the details of their reactivity towards  $\{\text{UO}_2\}^{2+}$  (and other metal ions), then there will be hope to realize the mining of the world's oceans in this century.

### 5. Synthetic and Structural Studies on Uranyl-Amidoxime Complexes and Their Technological Implications

As mentioned in Section 1, this report will concentrate mainly on the solid-state structures of uranyl complexes with small amidoxime mimics as ligands. Solution studies and complexes with competing metal ions will be briefly described. The structural formulae and abbreviations of the free ligands for which  $\{\text{UO}_2\}^{2+}$  complexes have been structurally characterized are presented in Figure 7. The number of hydrogen atoms in the abbreviations denotes the potentially acidic ones, including one H atom of the  $-\text{NH}_2$  group, which may be deprotonated [59]. The coordination modes of the neutral and anionic ligands that have been found to be present in the uranyl complexes are illustrated in Figure 8. Table 1 lists the characterized complexes.

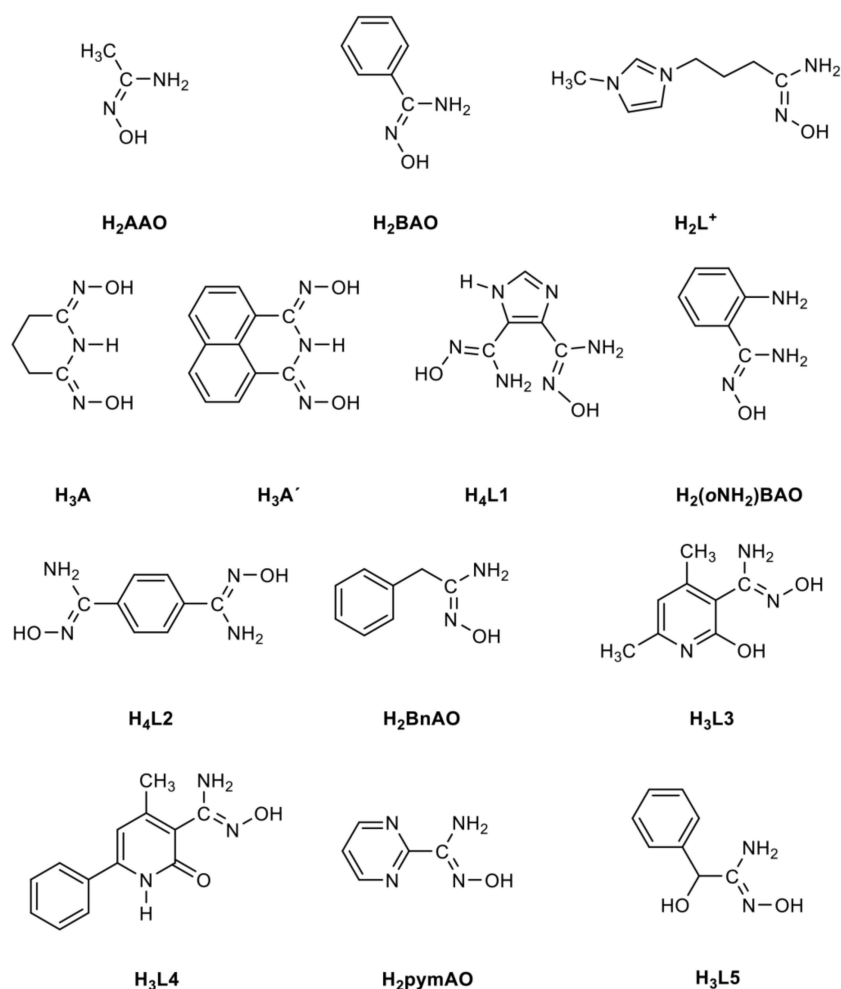


**Figure 7.** Structural formulae and abbreviations of the free ligands, the uranyl complexes of which have been structurally characterized by single-crystal X-ray crystallography. The carbon atoms of the amidoxime and methyl groups have been drawn with their symbol (C), while the other carbon atoms are drawn with the usual organic convention. The rationale behind the number of acidic hydrogen atoms is explained in the text.



**Table 1.** Structurally characterized uranyl complexes with amidoxime- and amidoximate-based ligands.

Complex Number	Formula <sup>1,2</sup>	Coordination Mode <sup>3,4</sup>	Refs.
1	[UO <sub>2</sub> {H <sub>2</sub> AAO(T)} <sub>4</sub> (NO <sub>3</sub> ) <sub>2</sub> ]	1.10	[75]
2	[UO <sub>2</sub> (NO <sub>3</sub> ) <sub>2</sub> {H <sub>2</sub> AAO(T)}](H <sub>2</sub> O)	1.10	[76]
3	[UO <sub>2</sub> (NO <sub>3</sub> ) <sub>2</sub> {H <sub>2</sub> AAO(T)} <sub>2</sub> ]	1.10	[76]
4	[UO <sub>2</sub> (HAAO) <sub>2</sub> (MeOH) <sub>2</sub> ]	1.110	[77]
5	[UO <sub>2</sub> {H <sub>2</sub> BAO(T)} <sub>4</sub> (NO <sub>3</sub> ) <sub>2</sub> ]	1.10	[75]
6	[(UO <sub>2</sub> ) <sub>4</sub> (O) <sub>2</sub> {H <sub>2</sub> BAO(T)} <sub>8</sub> (H <sub>2</sub> O) <sub>2</sub> ](NO <sub>3</sub> ) <sub>4</sub>	1.10, 2.20	[76]
7	[(UO <sub>2</sub> ) <sub>4</sub> (O) <sub>2</sub> {H <sub>2</sub> BAO(T)} <sub>10</sub> Na(NO <sub>3</sub> ) <sub>2</sub> ](NO <sub>3</sub> ) <sub>3</sub>	1.10, 2.20	[76]
8	[UO <sub>2</sub> (HBAO) <sub>2</sub> (MeOH) <sub>2</sub> ]	1.110	[76,77]
9	[(UO <sub>2</sub> ) <sub>3</sub> (NO <sub>3</sub> ) <sub>3</sub> (HBAO) <sub>3</sub> ]	1.110	[76]
10	[UO <sub>2</sub> (NO <sub>3</sub> ) <sub>2</sub> (HL)]	1.1100	[78]
11	[UO <sub>2</sub> (H <sub>2</sub> A) <sub>2</sub> ]	1.111	[79]
12	[UO <sub>2</sub> (H <sub>2</sub> A')(NO <sub>3</sub> )(MeOH)]	1.111	[80]
13	[UO <sub>2</sub> (H <sub>2</sub> L1)(H <sub>2</sub> O) <sub>2</sub> ]	1.11110000	[81]
14	[UO <sub>2</sub> {oNH <sub>2</sub> }BAO] <sub>2</sub> (MeOH) <sub>2</sub> ]	1.1100	[82]
15	{[(UO <sub>2</sub> ) <sub>4</sub> (O) <sub>2</sub> {H <sub>4</sub> L2(T)} <sub>3</sub> (H <sub>2</sub> L2)(H <sub>2</sub> O) <sub>2</sub> ]Cl <sub>2</sub> ] <sub>n</sub>	3.2110, 4.2200, 2.110000	[83]
16	[(UO <sub>2</sub> ) <sub>2</sub> (NO <sub>3</sub> ) <sub>4</sub> {H <sub>2</sub> BnAO(T)} <sub>2</sub> ]	2.20	[84]
17	[(UO <sub>2</sub> ) <sub>2</sub> (NO <sub>3</sub> ) <sub>2</sub> (H <sub>2</sub> L3) <sub>2</sub> ]	2.11100	[24]
18	[(UO <sub>2</sub> ) <sub>2</sub> HL3] <sub>2</sub> (DMSO) <sub>2</sub> ]	2.21110	[24]
19	[(UO <sub>2</sub> ) <sub>2</sub> (O <sub>2</sub> CMe) <sub>2</sub> (H <sub>2</sub> L4) <sub>2</sub> ]	2.11100	[24,25]
20	[(UO <sub>2</sub> ) <sub>2</sub> (HL4) <sub>2</sub> (DMSO) <sub>2</sub> ]	2.21110	[24,25]
21	[UO <sub>2</sub> (HpymAO) <sub>2</sub> (MeOH) <sub>2</sub> ]	1.11000	[24]
22	(Et <sub>3</sub> NH) <sub>2</sub> [(UO <sub>2</sub> ) <sub>3</sub> (O)(O <sub>2</sub> CMe) <sub>3</sub> (H <sub>2</sub> L5) <sub>3</sub> ]	2.2010	[25]

<sup>1</sup> The lattice solvent molecules are not written. <sup>2</sup> The symbol T in some *neutral* ligands suggests that the ligand is in the tautomeric form, not shown in Figure 7. <sup>3</sup> Using the Harris notation; the protonated, positively charged N atoms (which cannot form coordination bonds) are not represented in the notation. <sup>4</sup> The ligation modes are illustrated in Figure 8, along with the abbreviation of the coordinated ligands.

### 5.1. The Beginning of the Story and the Uranyl-Acetamidoxime and Uranyl-Benzamidoxime Chemistry

Acetamidoxime (H<sub>2</sub>AAO) and benzamidoxime (H<sub>2</sub>BAO) were the first amidoxime ligands used in uranyl chemistry [75]. Complexes [UO<sub>2</sub>{H<sub>2</sub>AAO(T)}<sub>4</sub>](NO<sub>3</sub>)<sub>2</sub> (**1**) and [UO<sub>2</sub>{H<sub>2</sub>BAO(T)}<sub>4</sub>](NO<sub>3</sub>)<sub>2</sub> (**5**) were prepared by the reactions of UO<sub>2</sub>(NO<sub>3</sub>)<sub>2</sub>·6H<sub>2</sub>O and ten (**1**) or four (**5**) equivalents of the ligands in EtOH and recrystallization from MeNO<sub>2</sub>; the yields are high (~90%). The symbol T in the neutral molecules suggests that the ligands are in their tautomeric form, not shown in Figure 7. The overall neutral ligands adopt the 1.10 coordination mode and the U<sup>VI</sup> atom is in a square bipyramidal environment (Figure 9).

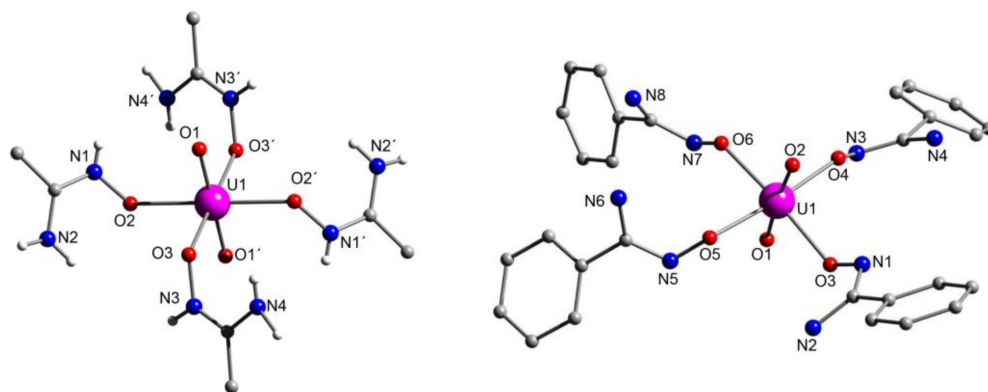


**Figure 9.** The molecular structures of the cations of complexes **1** (left) and **5** (right). For complex **5** (right) H atoms on the N atoms (N1, N2, N3, N4, N5, N6, N7 and N8) are not shown, as they have not been located in the crystal structure.

The  $\{\text{UO}_2\}^{2+}$ – $\text{H}_2\text{AAO}$  chemistry is not limited to compound **1**. Using a 1:1  $\text{H}_2\text{AAO}:\{\text{UO}_2\}^{2+}$  reaction ratio in EtOH, Forbes and co-workers isolated two complexes in which the nitrate ions (which are simply counterions in **1**) are coordinated [76]. Single-crystal X-ray crystallography revealed the mononuclear complexes  $[\text{UO}_2(\text{NO}_3)_2\{\text{H}_2\text{AAO}(\text{T})\}(\text{H}_2\text{O})]$  (**2**) and  $[\text{UO}_2(\text{NO}_3)_2\{\text{H}_2\text{AAO}(\text{T})\}_2]$  (**3**), where the ligand to metal ratios were 1:1 and 2:1, respectively (Figure 10). In both complexes, the amidoxime ligand adopts the tautomeric 1.10 mode (as in **1**) and the nitrate ligands are bidentate chelating, resulting in hexagonal bipyramidal geometries.

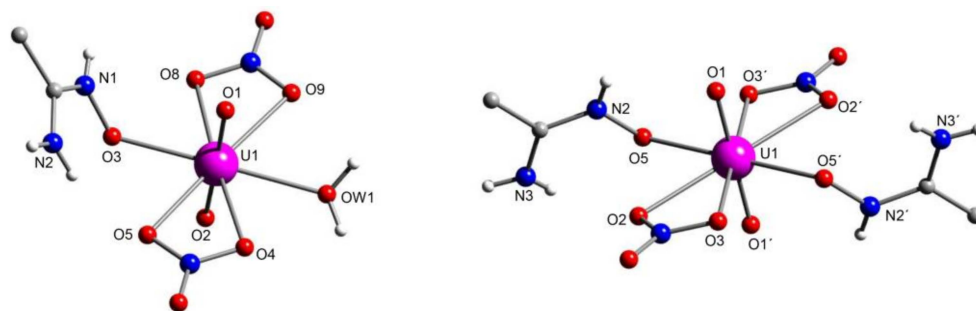


**Figure 10.** The molecular structure of complexes **2** (left) and **3** (right).

The Raman-active symmetric stretching vibration,  $\nu_s(\text{O}=\text{U}=\text{O})$ , appears at  $\sim 870\text{ cm}^{-1}$ . The peak matches with the value reported for  $\text{UO}_2(\text{NO}_3)_2 \cdot 6\text{H}_2\text{O}$ , suggesting a low electron density donation to the uranyl by the terminally coordinated amidoxime O atom [76].

To identify which binding mode is preferred when the amidoximate anion binds  $\{\text{UO}_2\}^{2+}$ , the Hay's group in the Oak Ridge National USA Laboratory performed Density Functional Theory (DFT) calculations to examine the configurations and relative stabilities of potential coordination motifs in a series of uranyl complexes containing acetamidoximate and aqua ligands [77]. The theoretical studies established the 1.110 or  $\eta^2$  (**d** in Figure 4) mode to be the most stable form. This prediction was confirmed by the structural characterization of compound  $[\text{UO}_2(\text{HAAO})_2(\text{MeOH})_2]$  (**4**), which was the first to have the  $\eta^2$  (1.110) motif (Figure 11). To keep the amidoxime moiety singly deprotonated,  $\text{Et}_3\text{N}$  was used in the reaction mixture, Equation (2). The  $\text{U}^{\text{VI}}$  center is in a hexagonal bipyramidal environment.

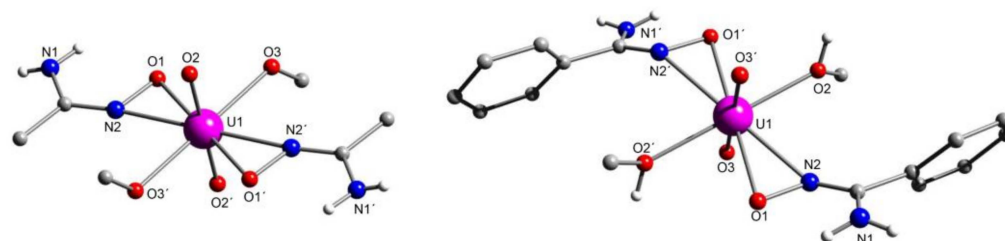
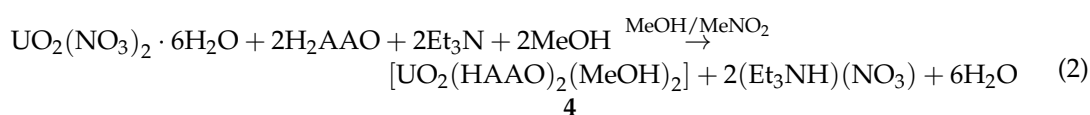


**Figure 11.** The molecular structures of complexes **4** (left) and **8** (right).

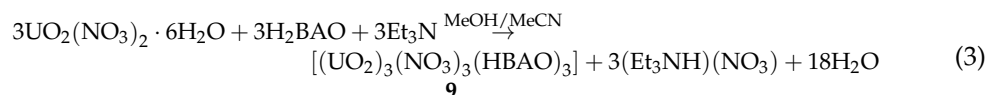
The findings of that seminal work were inconsistent with binding motifs that had been previously reported and suggested the possibility of the alternative  $\eta^2$  mode.

Vanadium exists in seawater at approximately 0.5–2 ppb (10–40 nM), which is similar to that of uranium (3.3 ppb, 13 nM). It is mainly present as V(V) species, due to slow oxidation of V(IV) by the oxygen dissolved in water; however,  $\sim 15\%$  is present in the V(IV) state as the vanadyl,  $\{\text{V}^{\text{IV}}\text{O}\}^{2+}$  moiety [85]. Thus, vanadium is one of the severely competing ions for  $\{\text{UO}_2\}^{2+}$  sorption. The interactions of  $\{\text{VO}\}^{2+}$  with  $\text{H}_2\text{AAO}$  were studied in aqueous solution by  $^1\text{H}$  and  $^{51}\text{V}$  NMR spectroscopy [85]. The results suggest irreversible

oxidation of V(IV) by H<sub>2</sub>AOO with the formation of acetamidine, CH<sub>3</sub>C(=NH)(NH<sub>2</sub>). The technological implication of the study is that V(IV) can react to permanently damage sites of the amidoxime-functionalized polymeric sorbents, thus significantly reducing the number of available sites for efficient uranyl uptake.

Complex [UO<sub>2</sub>{H<sub>2</sub>BAO(T)}<sub>4</sub>] (5, Figure 9) [75] was only the tip of the iceberg in the {UO<sub>2</sub>}<sup>2+</sup>–H<sub>2</sub>BAO chemistry. A reaction analogous to that described in Equation (2), but using H<sub>2</sub>BAO instead of H<sub>2</sub>AAO, gave complex [UO<sub>2</sub>(HBAO)<sub>2</sub>(MeOH)<sub>2</sub>] (8) [76,77]. The experimental reaction {UO<sub>2</sub>}<sup>2+</sup>:H<sub>2</sub>BAO ratio used was 1:4. Complex 8 has a similar molecular structure to that of the HAAO<sup>−</sup> analogue [UO<sub>2</sub>(HAAO)<sub>2</sub>(MeOH)<sub>2</sub>] (4) [77], Figure 9. The equatorial plane contains two HBAO<sup>−</sup> ligands *trans* to the uranium center, both ligands behaving in the side-on η<sup>2</sup> (1.110) mode, and two terminal MeOH molecules.

Compound [(UO<sub>2</sub>)<sub>3</sub>(NO<sub>3</sub>)<sub>3</sub>(HBAO)<sub>3</sub>] (9) [76] was prepared by the reaction represented in Equation (3); the solvent used was MeOH, but crystals were obtained by layering the reaction solution with MeCN. The experimental reaction {UO<sub>2</sub>}<sup>2+</sup>:H<sub>2</sub>BAO ratio was 1:1. Thus, the change of the solvent mixtures (MeOH for 8, MeOH/MeCN for 9), the experimental reaction ratios ({UO<sub>2</sub>}<sup>2+</sup>:ligand is 1:4 for 8 and 1:1 in 9) and the concentrations of the reaction solutions (high for 8 and low for 9) have a pronounced difference on the chemical and structural identity of the two products.



The molecular structure of 9 is shown in Figure 12. Each pair of almost linear {UO<sub>2</sub>}<sup>2+</sup> moieties is bridged by one 2.211 nitrato ligand, resulting in a triangular arrangement of the hexagonal bipyramidal U<sup>VI</sup> atoms. Each HBAO<sup>−</sup> ligand chelates one uranyl moiety in a 1.110 (η<sup>2</sup>) manner.

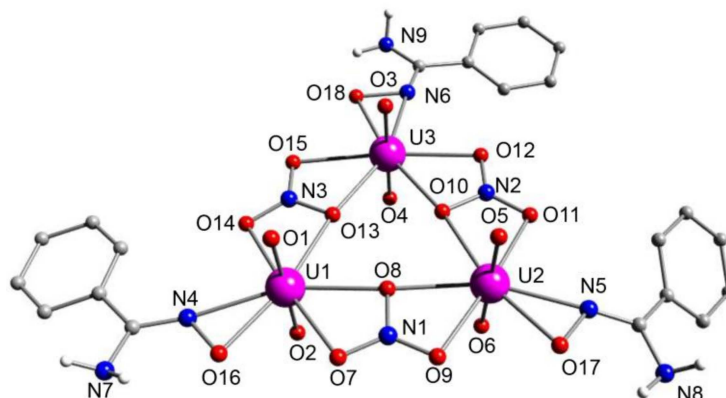
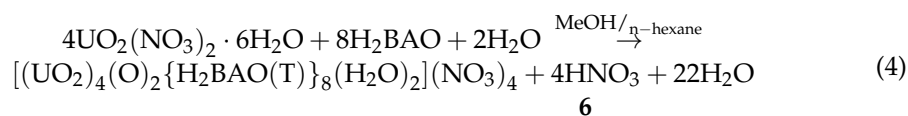
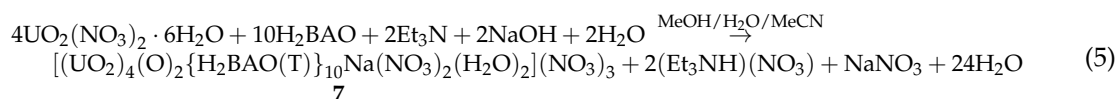


Figure 12. The molecular structure of the triangular complex 9.

Two remarkable uranyl hydrolysis products containing the overall neutral, tautomeric form of H<sub>2</sub>BAO have been synthesized [76]. These are [UO<sub>2</sub>]<sub>4</sub>(O)<sub>2</sub>{H<sub>2</sub>BAO(T)}<sub>8</sub>(H<sub>2</sub>O)<sub>2</sub>(NO<sub>3</sub>)<sub>4</sub> (6) and [(UO<sub>2</sub>)<sub>4</sub>(O)<sub>2</sub>{H<sub>2</sub>BAO(T)}<sub>10</sub>Na(NO<sub>3</sub>)<sub>2</sub>](NO<sub>3</sub>)<sub>3</sub> (7). The stoichiometric Equations (4) and (5) illustrate their preparations. The two extra H<sub>2</sub>O molecules in the reactants (in addition to those in the uranyl starting material) are written to show the hydrolysis process that leads to the two oxo (O<sup>2−</sup>) ligands.





Two points prompt comment. First, in both preparations the experimental  $\text{H}_2\text{BAO}:\{\text{UO}_2\}^{2+}$  ratio was 1:1. Second, the crystals of **6** appeared after 2 months, whereas those of **7** appeared in one day. It is obvious that the addition of aqueous NaOH speeds up the hydrolysis process. The structures of **6** and **7** are shown in Figures 13 and 14, respectively.

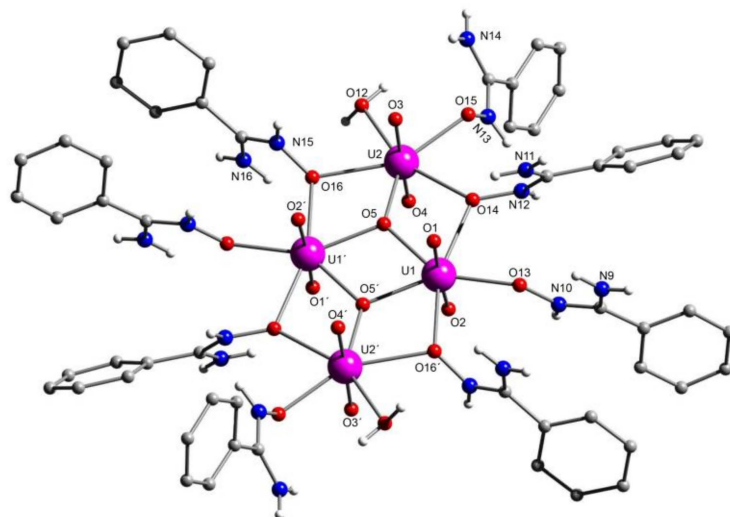


**Figure 13.** The molecular structure of one cation of complex **6**.

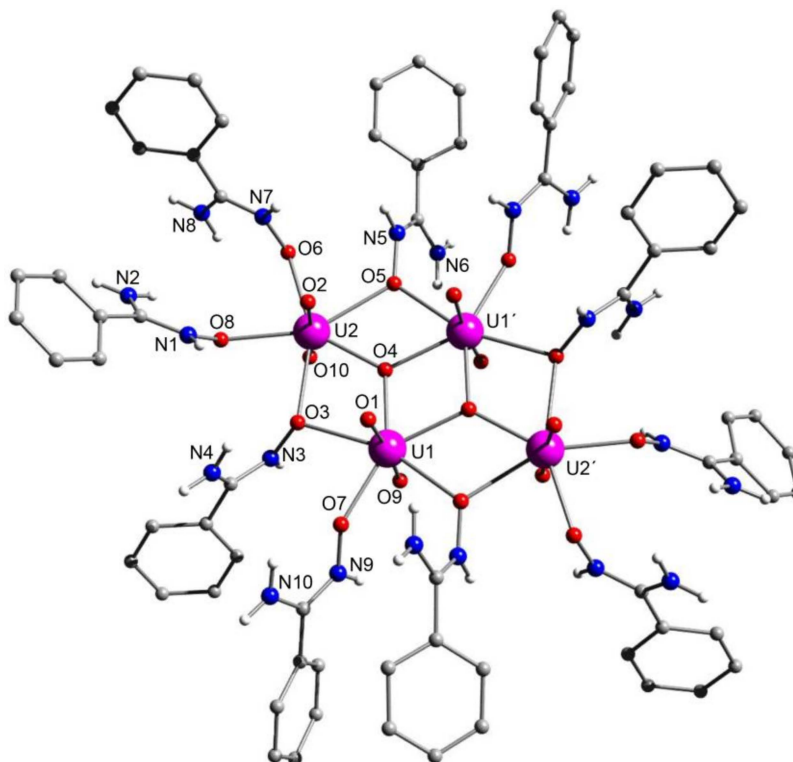


**Figure 14.** The tetranuclear cationic unit that is present in the crystal structure of **7**. The  $\{\text{Na}(\text{NO}_3)_2(\text{H}_2\text{O})_2\}^-$  unit that is located between the tetranuclear uranyl tetramers has not been drawn.

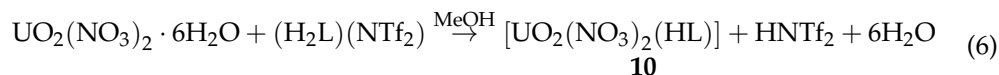
The crystal structure of **6** consists of two centrosymmetric, crystallographically independent, tetranuclear uranyl units that are structurally similar; only one of them is shown in Figure 13. Each tetranuclear unit has a  $\{U^{VI}_4(\mu_3-O)_2(\mu-OR)_4\}^{16+}$  core with a rhombus-like arrangement of the metal ions. There are eight  $H_2BAO$  ligands adopting their tautomeric (zwitterionic) form. Four behave as 1.10 ligands and four in the 2.20 manner. Two aqua ligands are coordinated to two uranyl moieties and thus each metal center has a pentagonal bipyramidal geometry. Compound **6** is a representative example of the hydrolysis products that would most likely be found on the surface of a  $\{UO_2\}^{2+}$ -amidoximated polyacrylonitrile mat [76].

Complex **7** could be either described as a coordination polymer (although it is not represented as such in Table 1) or as an ionic complex containing the cation  $[(UO_2)_4(O)_2(H_2BAO(T))_{10}]^{4+}$ , the anion  $[Na(NO_3)_2(H_2O)_2]^-$  and  $NO_3^-$  counterions in an 1:1:3 ratio. Overall, the tetranuclear unit of **7** is comparable to that of **6**, the only difference being the replacement of the two aqua ligands in the latter by two 1.10 zwitterionic forms of  $H_2BAO$  in the former. Since the  $[Na(NO_3)_2(H_2O)_2]^-$  unit, which contains two bidentate chelating nitrate groups, is located between neighboring uranyl tetramers interacting with them through  $\{UO_2\}^{2+} \cdots Na^+$  interactions [43], the compound can also be described as a coordination polymer. This type of interaction involves two "yl", i.e., oxo, oxygen atoms that belong to uranyl moieties of two neighboring tetramers, and can be represented as  $\{UO_2\}^{2+} \cdots Na^+ \cdots \{UO_2\}^{2+}$ . The experimental procedure for **7** [76] was aimed at reproducing the chemical conditions likely to exist on the surface of a  $\{UO_2\}^{2+}$ -amidoximated polyacrylonitrile mat, such as a hydrolytic environment (caused by NaOH), high metal to ligand molar ratios and low amounts of uranyl ions existing in dilute conditions. Solid-state Raman spectra of **6–9** showed impressive differences in the  $\nu_s(O=U=O)$  vibrations which depend on the coordination of the amidoxime group. The assignments from the solid-state spectra were used to deconvolute the solution Raman spectra of **6–9** (but also of **2** and **3**), giving valuable information for the uranyl- $H_2AAO/H_2BAO$  interactions in MeOH solutions at different metal to ligand ratios. At  $\{UO_2\}^{2+}:H_2AAO/H_2BAO$  ratios of 1:1 and 1:2, the dominant species in solution is the uranyl cation coordinated via the O atom of the oxime group (mode **c** or 1.100 in Figure 4). In contrast, at molar ratios of 1:3 and 1:4, the dominant species are a tetrameric uranyl- $\mu_3-O^{2-}$ -1.10 or/and 2.20 amidoxime (modes **b** or/and **h** in Figure 4) complex similar to compounds **6** and **7**, and an uranyl- $\eta^2$  (**d** in Figure 4) amidoxime complex similar to compounds **4**, **8** and **9**. Solid-state Raman spectra showed satisfactory agreement with Raman signals recorded from the  $\{UO_2\}^{2+}$ -amidoximated polyacrylonitrile mats; the detailed analysis demonstrated that the binding motif of the uranyl-amidoxime interaction in **6** and **7** better represent the uranyl species on the surface of the mats.

### 5.2. Incorporation of an Amidoxime Coordination Site within a Hydrophobic Ionic Liquid (IL)

One of the difficulties of growing single crystals of vanadium(IV, V) and uranyl complexes with amidoxime ligands is their tendency to form polymeric complexes. Roger's group developed smart synthetic methods for growing single crystals from low-melting salts (Ionic Liquids, ILs) at high concentrations and converting ligands into IL forms [78]. Several ILs have advantages with respect to traditional solvents for f-element separations; these include radiolytic stabilities, low vapor pressures and low flammability. However, several mechanisms are operative during metal separations, such as cation-exchange, anion-exchange, solvation, etc. Cation and anion exchange processes are often followed by the loss or leaching of the IL into the other phase because of the exchange occurring with either the anion or cation of the IL itself. An ideal IL would participate in either a simple proton exchange or a neutral exchange. The employment of amidoxime IL ligands may lead to new structural types which cannot be found with conventional solvents. Amidoxime IL ligands might provide a new solvent medium for metal complex formation and, therefore, previously unseen metal-amidoxime binding modes can be found. Such modes could provide helpful insight into amidoxime selectivity. The IL  $(H_2L)^+(NTf_2)^-$  (the formula of

the cation is shown in Figure 7;  $\text{Ntf}_2^-$  is the bis(trifluoromethane)sulfonamide anion) was synthesized [78] by alkylation of 1-methylimidazole with 4-chlorobutanenitrile, giving the corresponding cationic cyano derivative with the chloride ion, which was treated with excess of  $\text{NH}_2\text{OH}$  in  $\text{H}_2\text{O}$ , leading to the amidoxinium chloride salt. The latter was then phase-separated with the addition of  $\text{Li}(\text{NTf}_2)$  and the  $(\text{H}_2\text{L})^+(\text{NTf}_2)^-$  IL as a molten salt was obtained.



Complex  $[\text{UO}_2(\text{NO}_3)_2(\text{HL})]$  (10) was prepared by the reaction shown in chemical Equation (6). The  $\text{U}^{\text{VI}}$  atom is in a hexagonal bipyramidal environment (Figure 15). The ligands in the equatorial plane are two bidentate chelating nitrate groups and one (1-(4-amidoximate)butyl-3-methyl-imidazolium molecule. The ligand HL adopts the coordination mode 1.1100 (Figure 8) with an  $\eta^2$  (1.110) ligation of the negatively charged amidoxime group (d in Figure 4). The presence of a lattice, i.e., uncoordinated,  $\text{H}_2\text{O}$  molecule per complex (the crystallographic formula is  $10 \cdot \text{H}_2\text{O}$ ) provides strong evidence for the preference of amidoximate coordination to the coordination of  $\text{H}_2\text{O}$ . It is interesting that the HL zwitterion adopts an all-*cis* confirmation of the propyl chain, which places the positively charged imidazolium group directly above one of the nitrate ligands.

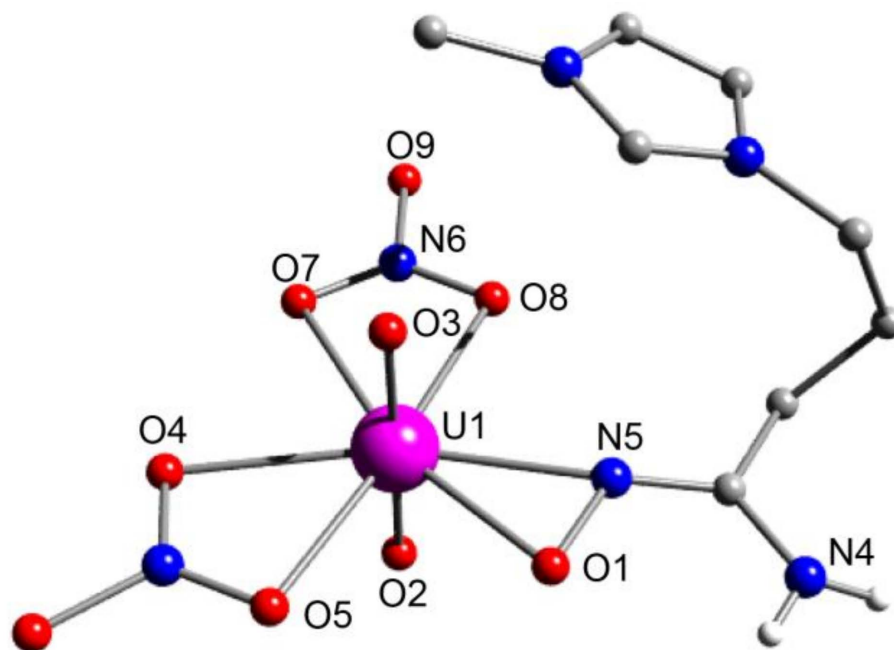


Figure 15. The molecular structure of 10.

Extensive studies in aqueous solution show high selectivity of the IL for  $\{\text{UO}_2\}^{2+}$  over  $\text{Th}^{4+}$  and  $\text{Eu}^{3+}$  [78]. This result (and similar studies with other amidoxime ILs) suggests that ILs could play a significant role in the separation processes of uranium from nuclear waste. Overall, the phase miscibility of  $(\text{H}_2\text{L})(\text{NTf}_2)$  with  $\text{H}_2\text{O}$ , extraction behavior, IR data and solid-state characterization support an  $\eta^2$  amidoximate ligation mechanism for the extraction of  $\{\text{UO}_2\}^{2+}$  from aqueous media.

### 5.3. Closed-Ring Glutarimidedioxime, Closed-Ring Glutarimidoxioxime, or Open-Chain Glutardiamidoxime Motifs? Structural and Solution Studies

Based on a variety of studies [11,27] using functionalized resins, scientists have obtained strong evidence that three types of amidoxime groups could form in the synthesis of the sorbent (Figure 6), and that the closed-ring glutarimidedioxime unit could be more

effective than the open-chain diamidoxime unit. In order to test this evidence, Teat, Rao and co-workers synthesized and fully characterized the ligand  $H_3A$  (Figure 7) [79]. The synthesis was achieved by the 1:2 reaction of glutaronitrile and  $H_2NOH$  in EtOH/ $H_2O$  at 80–90 °C for 5 days; the authors reported yields higher than 90%. This ligand can be considered as a small water-soluble analogue of the closed-ring cyclic imidedioxime sorbents (Figure 6), which have been proposed as the real units for the selective removal of  $\{UO_2\}^{2+}$  from seawater. Pale brown crystals of  $[UO_2(H_2A)_2]$  (**11**) were obtained by slow evaporation from  $H_2O$  containing high concentrations of  $\{UO_2\}^{2+}$  and  $H_3A$  (1:2) at pH 6–7 [79].

Two are the salient features of the structure of **11** (Figure 16). First, the H atoms of both oxime groups have been transferred from oxygen to N atoms. Second, the middle imide group has been deprotonated, resulting in an overall  $-1$  charge for the ligand ( $H_2A^-$ ). The two ligands are coordinated in the 1.111 mode (Figure 8). The re-arrangement of the H atoms of the oxime functional groups and the deprotonation of the imide group lead to a conjugated system with delocalized electron density on the  $(-O-N-C-N-C-N-O-)$  backbone, which coordinates preferentially and strongly to  $\{UO_2\}^{2+}$  in the equatorial plane.

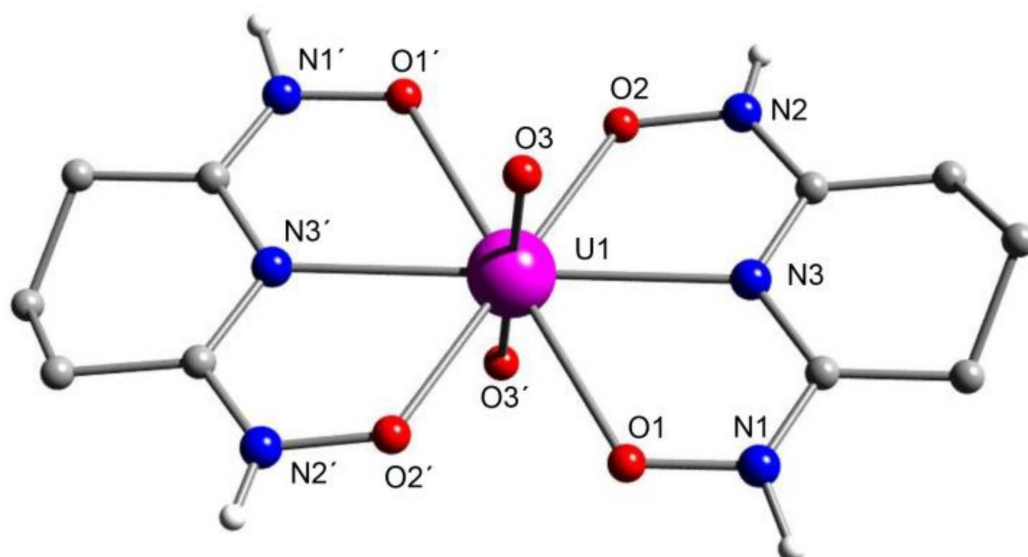


**Figure 16.** The molecular structure of **11**.

DFT geometry optimization was performed, and the calculated bond lengths are in rather good agreement with the experimental values; some differences have been attributed to crystal packing effects. Study of the stability constants reveals the formation of five uranyl species, namely  $UO_2(H_2A)^+$ ,  $UO_2(HA)$ ,  $UO_2(H_2A)_2$ ,  $UO_2(HA)(H_2A)^-$  and  $UO_2(HA)_2^{2-}$ . As stated in Section 4, under the conditions of seawater (pH~8.3), the main uranyl species is the stable complex  $[UO_2(CO_3)_3]^{4-}$ . It is thus logical that an effective sequestering ligand should be capable of replacing the carbonate groups. With the stability constants of  $U^{VI}$  for the formation of the species mentioned above and the constants of carbonate from the literature, the speciation of uranium under real seawater conditions ( $C_{[U]} = 3.3$  ppb,  $C_{carbonate} = 0.0023$  M) was calculated. At pH 8.3 and in the presence of 0.001 M  $H_3A$ , more than 95% of uranyl is complexed; the species present are  $UO_2(HA)(H_2A)^-$  (86%),  $UO_2(HA)_2^{2-}$  (8%) and  $UO_2(HA)$  (2%), suggesting that  $H_3A$  is a much stronger coordinating agent for  $U(VI)$  than that of  $CO_3^{2-}$  at the pH of seawater [79]. The major overall reaction is as written in Equation (7). Using the enthalpy values for  $HCO_3^-$ ,  $[UO_2(CO_3)_3]^{4-}$ ,  $H_3A$  and  $UO_2(HA)(H_2A)^-$ , the enthalpy of reaction (7) is  $+16.7$  kJ mol $^{-1}$ . This indicates that the efficiency of complexation is enhanced as the temperature increases, a fact that was experimentally confirmed in the Japan marine experiments [27,79].



A similar structural type for the cyclic imidedioxime unit was crystallographically observed in complex  $[\text{UO}_2(\text{H}_2\text{A}')(\text{NO}_3)(\text{MeOH})]$  (**12**) [80], where  $\text{H}_2\text{A}'^-$  is the monoanion of 1,8-naphthalimide dioxime ( $\text{H}_3\text{A}'$ , Figure 7). The ligand was synthesized by the reaction of 1,8-dicyanonaphthalene and excess of an equimolar mixture of  $\text{H}_2\text{NOH}\cdot\text{HCl}$  and  $\text{KOH}$  in  $\text{H}_2\text{O}/\text{EtOH}$  (3:1) in an 80% yield. The 1:1 reaction between  $\text{UO}_2(\text{NO}_3)_2\cdot 6\text{H}_2\text{O}$  and  $\text{H}_3\text{A}'$  in  $\text{MeOH}$  at room temperature provided access to complex **12** in 45% yield. The use of an excess of  $\text{H}_3\text{A}'$  does not affect the chemical and structural identity of the product, and thus the 1:2 analogue of **11** could not be isolated. The equatorial plane of the hexagonal bipyramidal  $\text{U}^{\text{VI}}$  atom consists of the deprotonated imide nitrogen, and the two oximate oxygen atoms of the 1.111  $\text{H}_2\text{A}'^-$  ligand (Figure 8), with one bidentate chelating nitrate group and the terminal methanol molecule. As in **11**, the deprotonation of the central imide group and the re-arrangement of the oxime hydrogen atoms results in a delocalized (-O-N-C-N-C-N-O-) backbone, which behaves as a tridentate chelating unit [80].

Performing the reaction that led to  $\text{H}_3\text{A}$  [79], but using room temperature instead of 80–90 °C, the same group isolated the open-chain glutardiamidoxime ( $\text{H}_4\text{B}$ , Figure 17) in a >90% yield [86]. This ligand can be considered as a small water-soluble analogue of the open-chain diamidoxime unit on the sorbent (Figure 6). The study focused on the uranyl complexation of  $\text{H}_4\text{B}$  in comparison with  $\text{H}_3\text{A}$ .

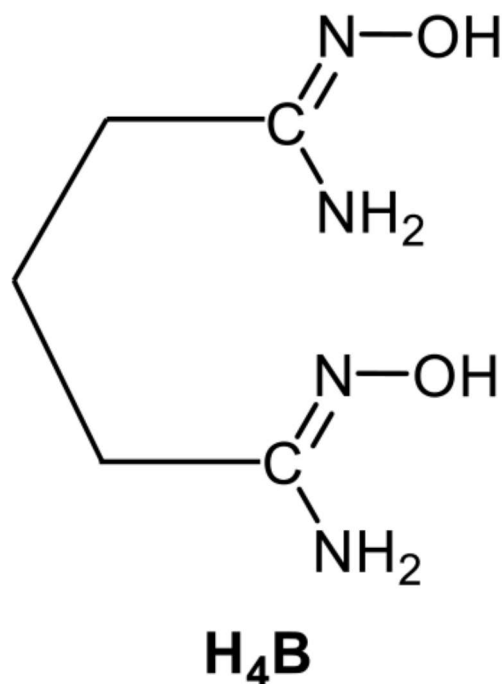


**Figure 17.** The structural formula of glutardiamidoxime and its abbreviation.

Uranyl complexes of  $\text{H}_4\text{B}$  or its anionic forms could not be crystallized for single-crystal X-ray structural studies. From a combination of potentiometric, spectrophotometric and microcalorimetric studies in 3%  $\text{NaCl}$  aqueous media, the following conclusions were drawn: (i) there are five species in solution, namely  $\text{UO}_2(\text{H}_2\text{B})$ ,  $\text{UO}_2(\text{H}_4\text{B})^{2+}$ ,  $\text{UO}_2(\text{H}_2\text{B})_2^{2-}$ ,  $\text{UO}_2(\text{H}_2\text{B})(\text{H}_3\text{B})^-$  and  $\text{UO}_2(\text{H}_4\text{B})_2^{2+}$ . (ii) In the  $\text{UO}_2(\text{H}_2\text{B})$  and  $\text{UO}_2(\text{H}_2\text{B})_2^{2-}$  complexes, the ligand is doubly deprotonated and the most probable ligation mode of  $\text{H}_2\text{B}^{2-}$  is depicted in Figure 18a; the deprotonation takes place at the two oxime groups. (iii) The probable coordination mode of the ligand in  $\text{UO}_2(\text{H}_4\text{B})^{2+}$  and  $\text{UO}_2(\text{H}_4\text{B})_2^{2+}$  is as shown in Figure 18b. (iv) Species  $\text{UO}_2(\text{H}_2\text{B})(\text{H}_3\text{B})^-$  has the  $\text{H}_2\text{B}^{2-}$  and  $\text{H}_3\text{B}^-$  ligands coordinated, as shown in Figure 18a.c. (v) Species with  $\eta^2$  (1.110, see Figure 4) coordination of the amidoximate groups were not proposed to exist in aqueous solution; this mode is present if the complexes are formed in non-aqueous environments. Thus, the solid-state structures of complexes with this mode—isolated from non-aqueous media, though highly valuable—are less

relevant concerning the  $\{\text{UO}_2\}^{2+}$  complexation in seawater. (vi) In the presence of 0.001 M concentrations of  $\text{H}_4\text{B}$  at pH 8.3, almost all uranyl is complexed by carbonato ligands, 98.6% as  $[\text{UO}_2(\text{CO}_3)_3]^{4-}$  and 1.2% as  $\text{UO}_2(\text{CO}_3)_2^{2-}$ . Only at pH values above 11,  $\text{H}_4\text{B}$  starts to compete  $\text{CO}_3^{2-}$  ions for complexing uranyl. (vii) Using an  $\text{H}_4\text{B}$  concentration of 0.01 M at pH 8.3,  $\sim 77\%$  of U(VI) is still complexed by carbonato groups, and only  $\sim 22\%$  is in the form of  $\text{UO}_2(\text{H}_2\text{B})(\text{H}_3\text{B})^-$ . Summarizing the results from the information provided in references [79,86], it is obvious that  $\text{H}_3\text{A}$  is much stronger complexing agent than  $\text{H}_4\text{B}$ , and can be very effectively compete with  $\text{CO}_3^{2-}$  ions for uranyl at the seawater pH. Thus, it seems that the cyclic glutarimidodioxime units (as modelled by  $\text{H}_3\text{A}$ ) are the preferred configuration for the capture of  $\{\text{UO}_2\}^{2+}$  from seawater. The technological implications of the above results in this section (5.3) are that improvement of the capability of the sequestration of uranyl from seawater requires high temperatures (80–90 °C) in the grafting/reaction process for the preparation of amidoxime-based sorbents, because these temperatures result in a higher percentage of the cyclic (closed-ring) imidedioxime units.

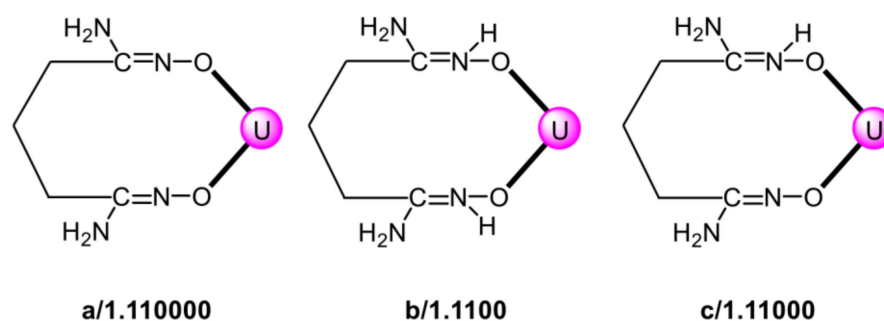


**Figure 18.** The probable coordination modes of  $\text{H}_2\text{B}^{2-}$  (a),  $\text{H}_4\text{B}$  (b) and  $\text{H}_3\text{B}^-$  (c) in the uranyl-complexes that form in 3% NaCl aqueous solution using glutardiamidoxime ( $\text{H}_4\text{B}$ ) as ligand at the pH of seawater (8.3). The coordination bonds have been drawn as bold lines.

Performing the reaction that led to  $\text{H}_3\text{A}$  [79], but using a large excess of glutaronitrile to hydroxylamine ratio (10:1), the group led by Rao synthesized glutarimidoxioxime ( $\text{H}_2\text{C}$ , Figure 19) [11]. This ligand can be considered a small water-soluble analogue of the closed-ring imidoxioxime unit on the sorbent (Figure 6). The study focused on the uranyl complexation of  $\text{H}_2\text{C}$  in comparison with  $\text{H}_3\text{A}$  and  $\text{H}_4\text{B}$ .

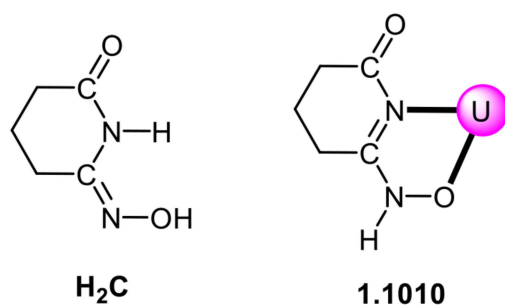


**Figure 19.** The structural formula of glutarimidoxioxime and its abbreviation (left), and the proposed coordination mode of  $\text{HC}^-$  in the dominant species  $\text{UO}_2(\text{HC})^+$  (right). The coordination bonds have been drawn as bold lines.

As in the case of  $\text{H}_4\text{B}$ , no uranyl complexes of  $\text{H}_2\text{C}$  (or its anionic forms) could be crystallized for single-crystal X-ray elucidation of their structures. Speciation models based on thermodynamic data indicated that, compared with  $\text{H}_3\text{A}$  and  $\text{H}_4\text{B}$ ,  $\text{H}_2\text{C}$  forms a much weaker complex with the uranyl cation,  $\text{UO}_2(\text{HC})^+$ , even at a high ligand:uranium(VI) reaction ratios (3:1, 4:1). The weaker binding ability of  $\text{H}_2\text{C}$  than that of  $\text{H}_3\text{A}$  has been explained in terms of the lower denticity of the former. The  $\text{UO}_2(\text{HC})^+$  species cannot effectively compete with the hydrolysis equilibria of  $\{\text{UO}_2\}^{2+}$  in slightly acidic to neutral

solutions, or the complexation of this cation with  $\text{CO}_3^{2-}$  ions in neutral to alkaline solutions. It was proposed that  $\text{HC}^-$  adopts the bidentate chelating mode 1.1010 (Figure 19, right), a conclusion that was supported by DFT computation [11]. The bidentate coordination seems to be stabilized by the formation of an H bond with one  $\text{H}_2\text{O}$  from the coordination sphere of  $\{\text{UO}_2\}^{2+}$  as donor and the carbonyl O atom of  $\text{HC}^-$  as acceptor. The technological implications of the results with  $\text{H}_2\text{C}$  are similar to those in the studies with  $\text{H}_3\text{A}$  and  $\text{H}_4\text{B}$ . These three ligands are models of the three functionalities that could be formed in the radiation-induced grafting process to prepare the sorbent materials for the extraction of the uranyl ion from seawater. The results suggest that the conditions of the process, such as the temperature and the reactants' ratio, must be very carefully selected and optimized to maximize the formation of the closed-ring imidedioxime units (represented by  $\text{H}_3\text{A}$ ), and minimize the formation of the open-chain diamidoxime (represented by  $\text{H}_4\text{B}$ ) and closed-ring imidoxioxime (represented by  $\text{H}_2\text{C}$ ) units; in particular, the binding strength of  $\text{H}_2\text{C}$  with  $\{\text{UO}_2\}^{2+}$  is eight orders of magnitude lower than that of the other two cases.

#### 5.4. Structural Clues to $\{\text{UO}_2\}^{2+}/\{\text{V}^{\text{V}}\text{O}_2\}^+$ Competition in Seawater Extraction Using Amidoxime-Based Sorbents

As mentioned in Section 5.1, one of the greatest disadvantages of the amidoxime sorbent materials for the recovery of  $\{\text{UO}_2\}^{2+}$  from seawater is the competition with the vanadium species  $\{\text{V}^{\text{IV}}\text{O}\}^{2+}$  and  $\{\text{V}^{\text{V}}\text{O}_2\}^+$  [85]; these species reduce the uranyl capacity by strong binding that stripping them irreversibly damages the sorbent. The knowledge of whether uranium and vanadium interact with the same sites through the same or similar manners is a critical question, the answer to which can improve the existing technology.

The group led by Rogers presented results, based on crystallography, in a seminal paper [81], which remains to date the only comparison in the solid state. They studied the interactions of adjacent di(amidoxime) binding sites with  $\{\text{UO}_2\}^{2+}$  and  $\{\text{VO}_2\}^+$  ions by incorporating this unit in the small ligand  $\text{H}_4\text{L1}$  (Figure 7). This compound was synthesized in  $\text{MeOH}/\text{H}_2\text{O}$  under refluxing conditions by the reaction of the commercially available 4,5-dicyanoimidazole and a large excess of  $\text{H}_2\text{NOH}$ .

The compound  $\text{H}_4\text{L1}$  was reacted with aqueous solutions of  $\text{UO}_2(\text{NO}_3)_2 \cdot 6\text{H}_2\text{O}$  and  $\text{V}_2\text{O}_5$  providing access to complexes  $[\text{UO}_2(\text{H}_2\text{L1})(\text{H}_2\text{O})_2]$  (**13**, Table 1) and  $[(\text{VO}_2)_2(\text{H}_3\text{L1})_2]$  (**II**), respectively. The molecular structures of the complexes are shown in Figures 20 and 21. In the structure of **13** there are two crystallographically independent, but structurally similar molecules. The ligand is deprotonated at both amidoxime  $-\text{OH}$  groups, allowing both amidoximate groups to coordinate in the  $\eta^2$  (1.110) mode (mode **d** in Figure 4). The overall ligation mode of  $\text{H}_2\text{L1}^{2-}$  is 1.11110000 (Figure 8). The  $\text{U}^{\text{VI}}$  atom is in a hexagonal bipyramidal environment with additional coordination of two aqua ligands.

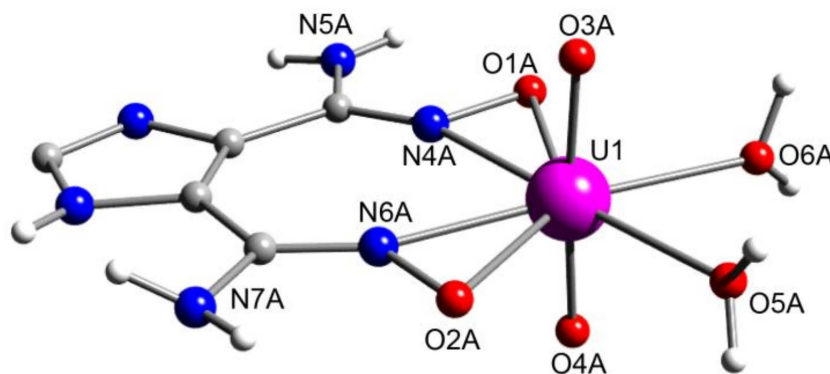


**Figure 20.** The structure of one of the two crystallographically independent uranyl molecules that are present in the crystal of **13**.

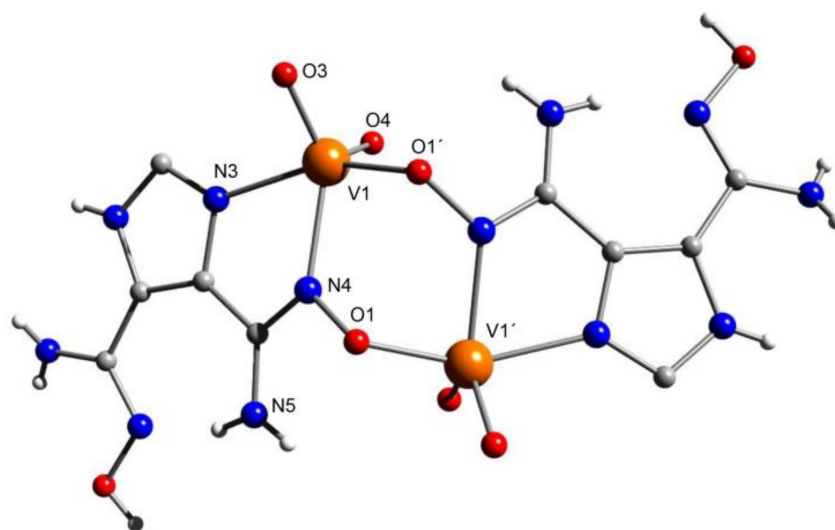


**Figure 21.** The molecular structure of **II**.

Complex **II** is dinuclear. Two *cis*  $\{VO_2\}^+$  units are bridged by the deprotonated oximate groups, each of which belongs to a  $H_3L1^-$  ligand; the latter adopts the 2.10110000 mode illustrated in Figure 22. Thus, the ligand is deprotonated at a single oxime O atom and coordinates to one  $V^V$  atom only through this oxygen, while both the oximate and pyridine-type imidazole N atoms coordinate to the other metal center.

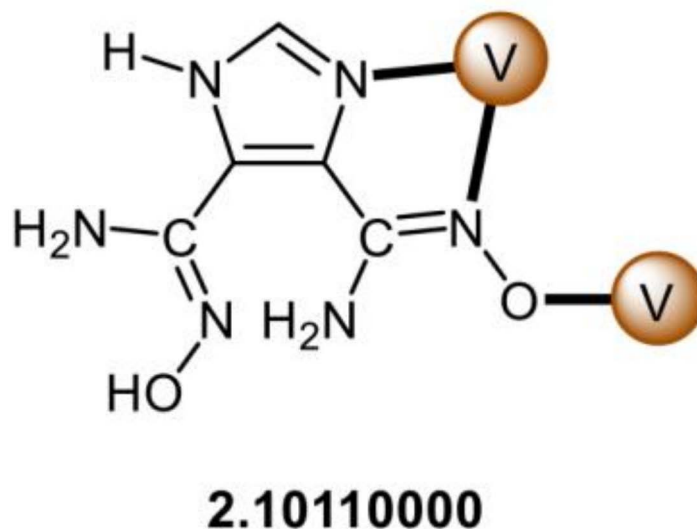


**Figure 22.** The coordination mode of  $H_3L1^-$  in complex **II**. The coordination bonds have been drawn with bold lines.

Complexes **12** and **II** were isolated from saturated solutions. This shows that for both  $\{UO_2\}^{2+}$  and  $\{VO_2\}^+$ , the ligand is able to coordinate in  $H_2O$ . However, the two structures differ, mainly in the manner the oxime groups interact with the metal ions. Generally, the functionalization of the R group in the amidoxime-functionalized polymers has not received attention. If the R group is key to the difference observed between the structures of **12** and **II**, then the modification of the R group could result in greater control of the metal selectivity of amidoxime-functionalized polymers without compromising affinity for  $\{UO_2\}^{2+}$ .

The problem of  $\{UO_2\}^{2+}/V(IV,V)$  competition has been addressed also in solution by a number of experimental and theoretical methods, with sometimes contradictory conclusions. From a number of carefully designed studies [87–91], we briefly comment on that of reference [87]. A complementary and detailed study combined *ab initio* simulations with

thermochemical data and XAFS spectroscopy was performed to elucidate the strong and selective binding of V by polyamidoximes. While the open-chain diamidoxime functionalities (Figure 6a) do not bind V, the closed-ring (cyclic) imidedioxime group (Figure 6b, left) of the adsorbent forms a peculiar non-oxo V(V) complex, in which the metal ion is bound in a tridentate chelating fashion to two fully deprotonated cyclic imidedioxime units, forming a highly distorted octahedral complex. The complex exhibits a very high stability constant value. XAFS studies of adsorbents after deployment in environmental seawater confirm vanadium binding solely by the cyclic imidedioxime groups; thus, this unit is solely responsible for the very strong sorption of vanadium by polyamidoxime sorbent materials. The much higher stability of the non-oxo V(V) complex compared to the uranyl complex with cyclic imidedioxime explains why  $\{UO_2\}^{2+}$  cannot access the imidedioxime sorption sites that are occupied by vanadium. Additionally, the broad pH region in which the V(V) species is stable can explain the difficulty of removing vanadium from amidoxime sorbents during the elution process, even under acidic conditions. The authors concluded that the selectivity of polyamidoxime sorbents for U(VI) and V(V) would be increased by reducing the cyclic imidedioxime moiety. Another, final point of interest is the negative enthalpy of the reaction that forms the non-oxo V(V) complex under the conditions of seawater, and this means less sorption of this metal ion at higher temperatures, in contrast with the sorption of  $\{UO_2\}^{2+}$ , which increases as the temperature increases. The opposing effects of temperature on the sorption of these metal ions could be exploited for the achievement of optimal extraction.

#### 5.5. Bio-Inspired Nano-Traps for Uranyl Extraction

An innovative approach for the regulation of uranyl capture has been proposed by Ma and co-workers [82]. It is based on the creation of bio-inspired nano-traps, which includes construction of chelating groups into porous frameworks, where the binding motif's interaction towards  $\{UO_2\}^{2+}$  is enhanced by the incorporation of an assistant group, like in biological systems. As an example, a porous framework possessing 2-aminobenzamidoxime ( $H_2(oNH_2)BAO$ , Figure 7) is excellent in sequestering high uranyl concentrations with good capacities ( $530 \text{ mg g}^{-1}$ ) and trace quantities, including this ion in real seawater ( $4.36 \text{ mg g}^{-1}$ , triple the benchmark). A detailed study involving spectroscopic studies and theoretical calculations has revealed that the amino substituent provides assistance in lowering the charge on uranyl and serves as a H bond acceptor, enhancing the overall affinity towards this ion. In the context of these studies, complex  $[UO_2\{H(oNH_2)BAO\}_2(MeOH)_2]$  (14) was structurally characterized (Figure 23). The  $U^{VI}$  atom is in a hexagonal bipyramidal environment with the singly deprotonated ligand  $H(oNH_2)BAO^-$  adopting the 1.1100 mode (Figure 8); the deprotonated amidoxime group participates in the 1.110 or  $\eta^2$  manner (d in Figure 4). Furthermore, the molecule is stabilized by relatively strong intermolecular H bonds, with the MeOH oxygens as donors and the *ortho*  $-NH_2$  nitrogens as acceptors. DFT calculations suggest that the H bonds are retained in the absence of crystal packing forces.

#### 5.6. An Uranyl MOF Containing a Partially Hydrolyzed Tetranuclear Mode from the Use of a Diamidoxime Ligand

The group led by Rogers [83] investigated the reactions of the uranyl cation and 1,4-(diamidoximyl)benzene ( $H_4L2$  in Figure 7) in order to understand electronic and cooperativity effects on the coordination chemistry of the amidoxime group. There are two amidoxime groups in the molecule separated by an aromatic spacer, which would be tautomerized to their zwitterionic forms. It was expected that the amidoxime groups would not significantly influence each other's coordination.  $H_4L2$  was synthesized by the reaction of  $H_2NOH$  with commercially available 1,4-dicyanobenzene. Compound  $\{[UO_2]_4(O)_2(H_4L2(T))_3(H_2L2)(H_2O)_2\}Cl_2\}_n$  (15 or UMOFUA) was prepared from the reaction represented by Equation (8). The two extra  $H_2O$  molecules in the reactants (in addition to those in the uranyl starting material) are written to show the hydrolysis process that leads to the two oxo ( $O^{2-}$ ) ligands.

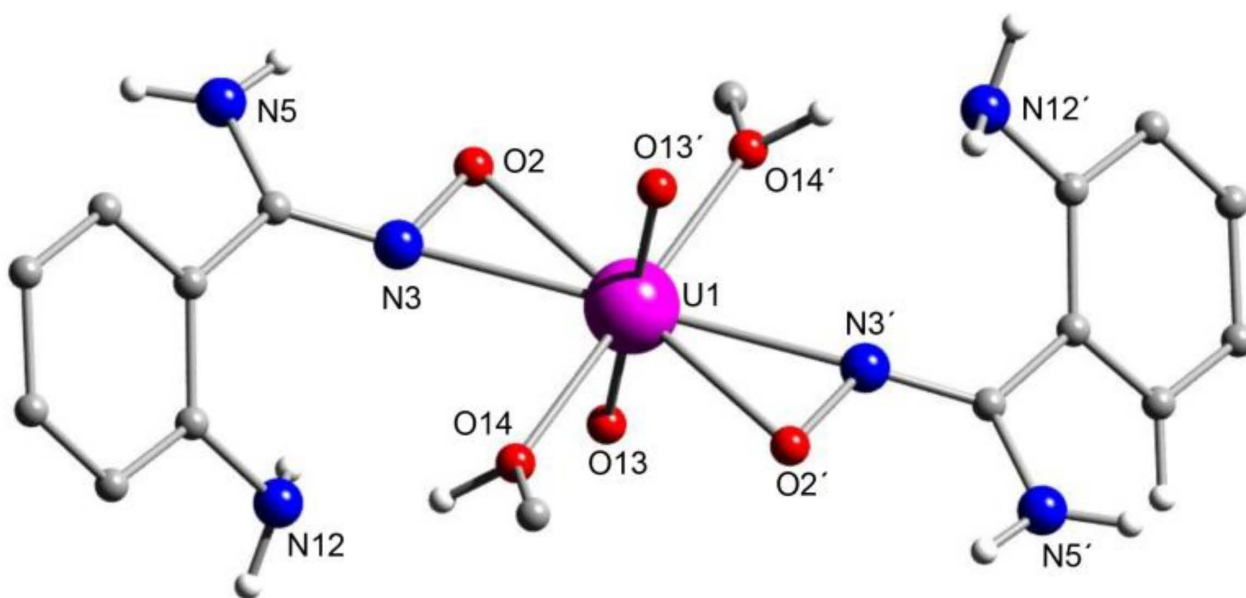
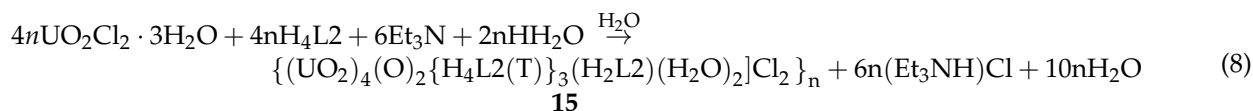
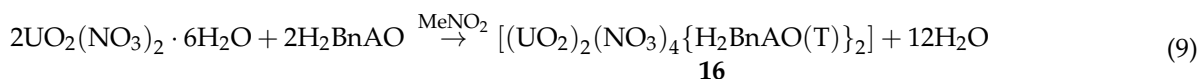


**Figure 23.** The molecular structure of 14.

The complex is a non-interpenetrated 3D Metal-Organic Framework (MOF). Ten lattice  $\text{H}_2\text{O}$  molecules and two  $\text{Cl}^-$  ions are inside the framework. The structure is constructed by planar  $\{\text{U}_4^{\text{VI}}(\mu_3\text{-O})_2(\mu\text{-OR})_4\}^{16+}$  cores surrounded by six  $\text{H}_4\text{L2}$  and two  $\text{H}_2\text{L2}^-$  ligands (Figure 24). The overall neutral, zwitterionic  $\text{H}_4\text{L2}(\text{T})$  molecules and the  $\text{H}_2\text{L2}^{2-}$  anions adopt three coordination modes illustrated in Figure 8. It is apparent that the deprotonated amidoxime groups of  $\text{H}_2\text{L2}^{2-}$  do not coordinate in the  $\eta^2$  (1.110) fashion. The geometry around the  $\text{U}^{\text{VI}}$  centers is pentagonal bipyramidal. The final conclusion of this work [83] is that it shows the possibility of tailoring even the strong uranyl amidoxime interaction for use as a valuable tool in preparing new amidoxime-functionalized materials.

#### 5.7. A Dinuclear Uranyl Complex with a Rare Bridging Zwitterionic-Amidoxime Group

The small number of uranyl-amidoxime complexes and the non-definite proof of a dominant binding motif shows the need for further structural studies of these complexes. The bridging zwitterionic amidoxime group (**h** or 2.20 in Figure 4) is rare in uranyl chemistry, and it has only been observed in complexes **6**, **7** and **15** (Table 1). Berryman and Decato prepared complex  $[(\text{UO}_2)_2(\text{NO}_3)_4\{\text{H}_2\text{BnAO}(\text{T})\}_2]$  (**16**) [84], where  $\text{H}_2\text{BnAO}$  is benzylamidoxime (Figure 7); the preparation is illustrated in Equation (9). This was the first structurally characterized dinuclear complex with any type of amidoxime/amidoximate ligation.



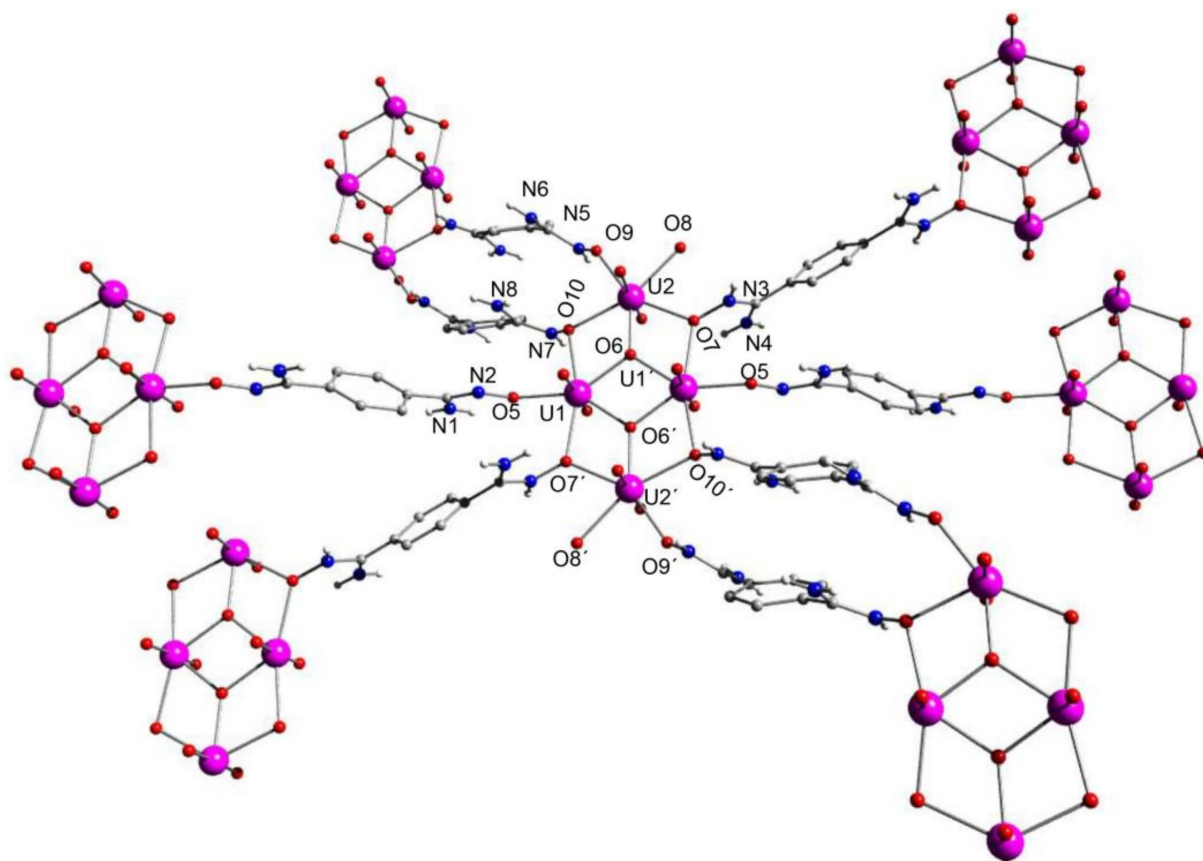


**Figure 24.** A portion of the 3D structure of the MOF 15.

The molecular structure of the complex is shown in Figure 25. The two uranyl moieties are doubly bridged by the negatively charged oxygen atom of the 2.20 overall neutral, tautomeric ligand (Figure 8). The  $U^{VI}$  centers adopt a distorted hexagonal bipyramidal geometry. The bidentate nitrate groups occupy *cis* positions in the equatorial plane, while the remaining sites are occupied by the bridging oxygen atoms. There is also one uncoordinated  $H_2O$  molecule per dimer in the lattice residing on a  $C_2$  axis. The similar  $C-N_{oxime}$  and  $C-N_{amino}$  bond lengths in the complex are indicative of resonance stabilization of the positive charge by the lone pair of electrons on the  $N_{amino}$  atom. DFT computations reveal that the dinuclear complex exhibits a shallow potential energy surface, which allows for the inclusion of a lattice  $H_2O$  molecule in the solid state. The study indicates that amidoxime tautomerization, before or after coordination with the uranyl cation, may influence the binding mode and selectivity of amidoximated polymeric materials, emphasizing the need for more coordination chemistry with small ligands in the pursuit of an in-depth understanding of the amidoxime selectivity for the uranyl ion.

### 5.8. Uranyl Complexes with New Amidoxime-Based Ligands

With a primary goal of studying the influence of the chemical nature and the charge of neighboring donor sites on the amidoxime coordinating behavior, and with a secondary goal to provide structural clues to  $\{UO_2\}^{2+}$ /vanadium competition, we have designed and synthesized the new ligands  $H_3L3$ ,  $H_3L4$  and  $H_3L5$ ; we have also used the known ligand  $H_2pmAO$  in reactions with uranyl starting materials. Some of the structurally characterized uranyl complexes are listed in Table 1. Since the results are unpublished, they will be discussed briefly [24,25].

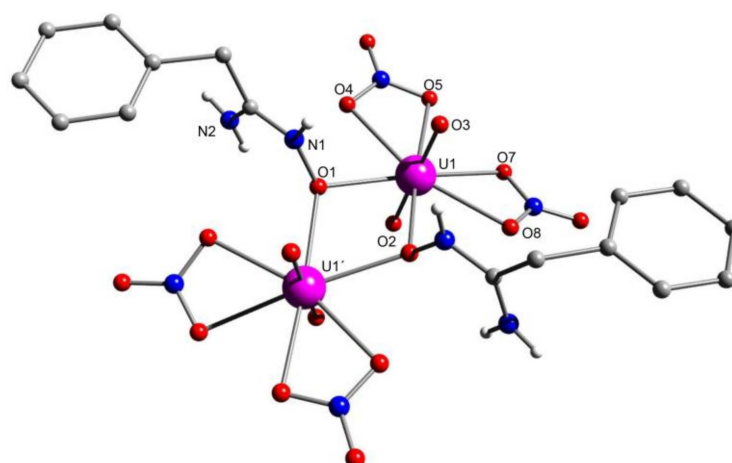


Figure 25. The molecular structure of 16.

The ligand H<sub>3</sub>L3 gives two dinuclear complexes with different deprotonation levels: [(UO<sub>2</sub>)<sub>2</sub>(NO<sub>3</sub>)<sub>2</sub>(H<sub>2</sub>L3)<sub>3</sub>] (17, Figure 26) and [(UO<sub>2</sub>)<sub>2</sub>(HL3)<sub>2</sub>(DMSO)<sub>2</sub>] (18, Figure 27). Similarly, H<sub>3</sub>L4 provides access to two analogous dinuclear complexes: [(UO<sub>2</sub>)<sub>2</sub>(O<sub>2</sub>CMe)<sub>2</sub>(H<sub>2</sub>L4)<sub>2</sub>] (19, Figure 28) and [(UO<sub>2</sub>)<sub>2</sub>(HL4)<sub>2</sub>(DMSO)<sub>2</sub>] (20, Figure 29). The four complexes have been prepared in organic solvents. The structures of the free ligands H<sub>3</sub>L3 and H<sub>3</sub>L4 have been also solved. In the solid state, the two organic compounds are in their enol (H<sub>3</sub>L3) and keto (H<sub>3</sub>L4) forms, while in DMSO, their enol forms dominate. The two ligands behave similarly towards the {UO<sub>2</sub>}<sup>2+</sup> ion (Figure 8), suggesting that the -Me/-Ph substitution has no effect on their coordination modes and the molecular structures of the resulting complexes. In complexes 17 and 19, the singly deprotonated ligands are in their terminally coordinated keto forms and adopt the 2.11100 coordination mode. In complexes 18 and 20, the doubly deprotonated ligands are in their bridging enolate forms, adopting the 2.21110 mode. In the complexes with the singly deprotonated ligands, the amidoximato(−1) group participates in the *syn, anti* 2.110 ( $\eta^1:\eta^1:\mu$ ) mode (**g** in Figure 4), with the oximato moiety providing the bridge between the two uranyl centers. Contrarily, in the complexes with the doubly deprotonated forms, the amidoximato(−1) group adopts the 1.110 or  $\eta^2$  (**d** in Figure 4) mode, resulting in the formation of the 3-membered chelating ring, with the enolato oxygen atom providing the monoatomic bridge between the two uranyl sites. Our results suggest that the behavior of the amidoximato(−1) group (chelating or bridging) depends on the nature and charge of the neighboring potential donor atom with which the amidoximato(−1), oximate-type nitrogen atom can participate in a stable 6-membered chelating ring.

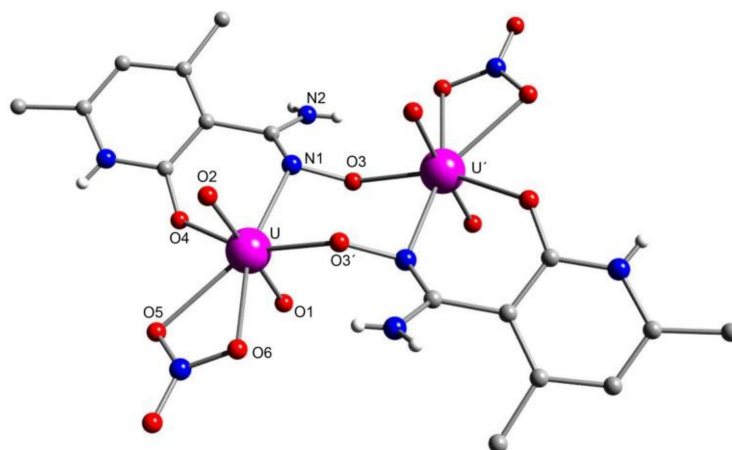


Figure 26. The molecular structure of 17.

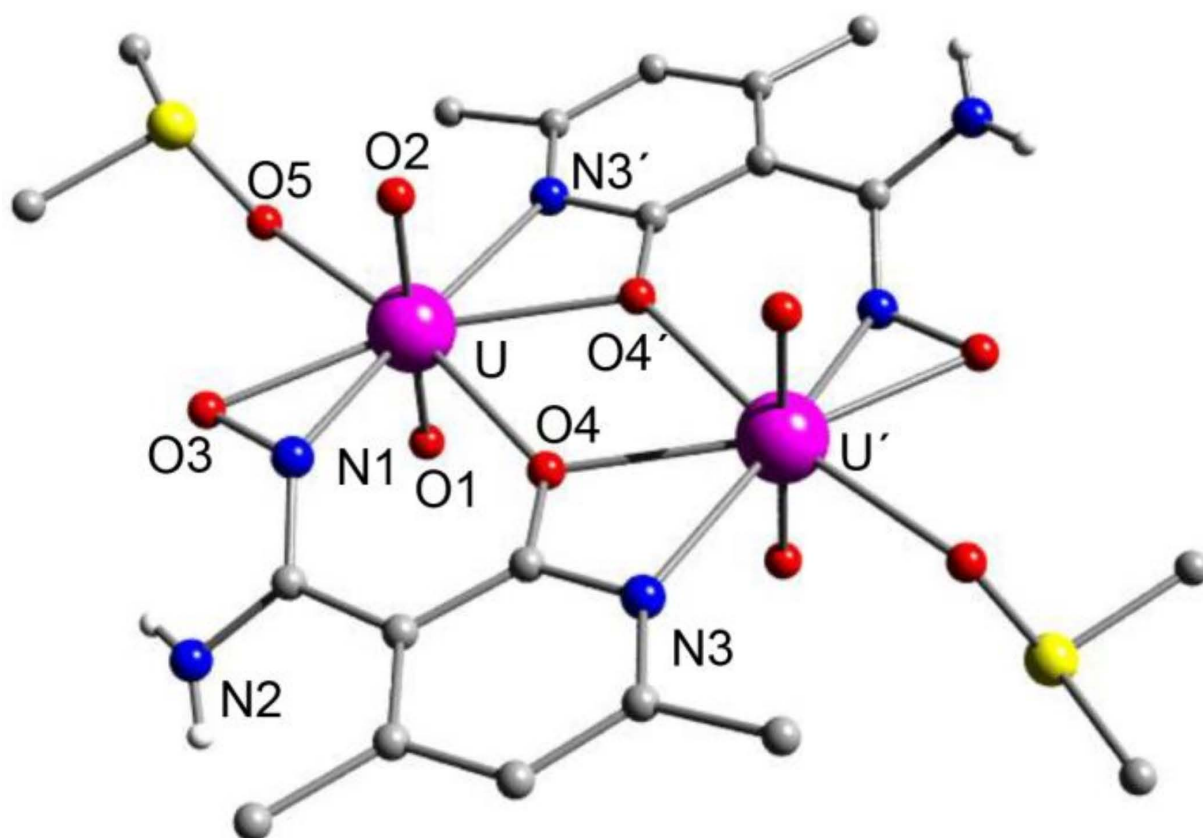


Figure 27. The molecular structure of 18.

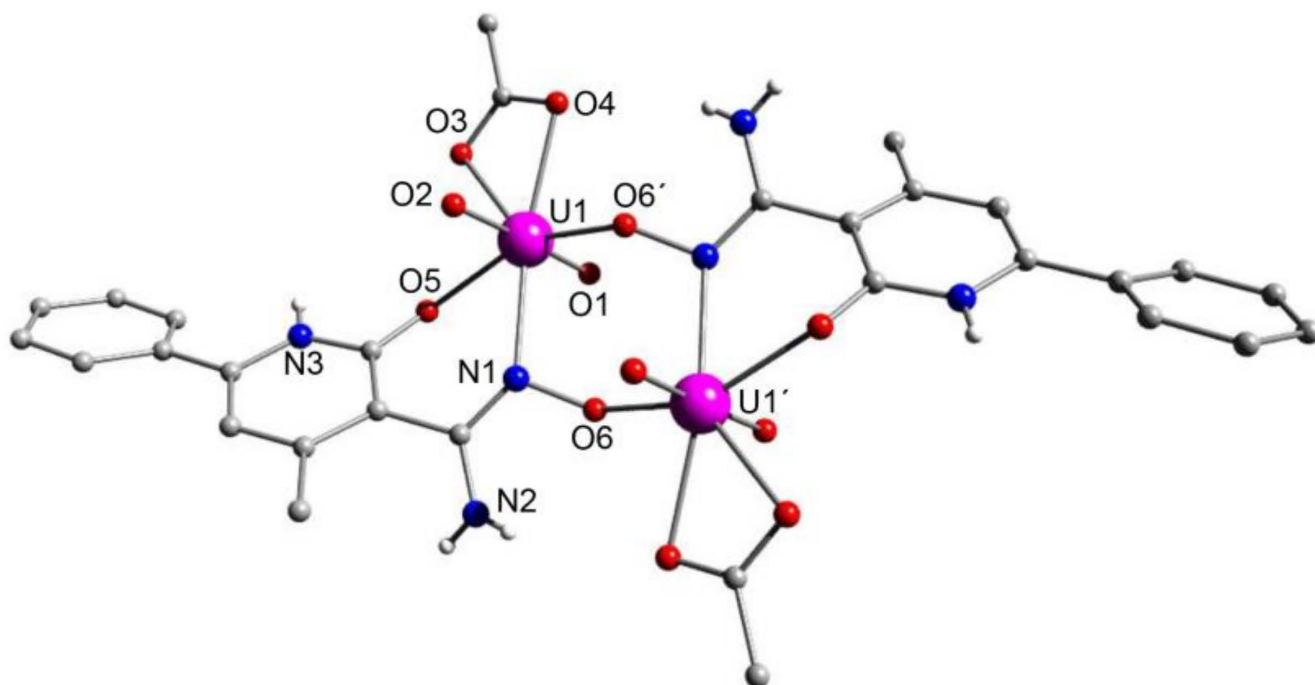
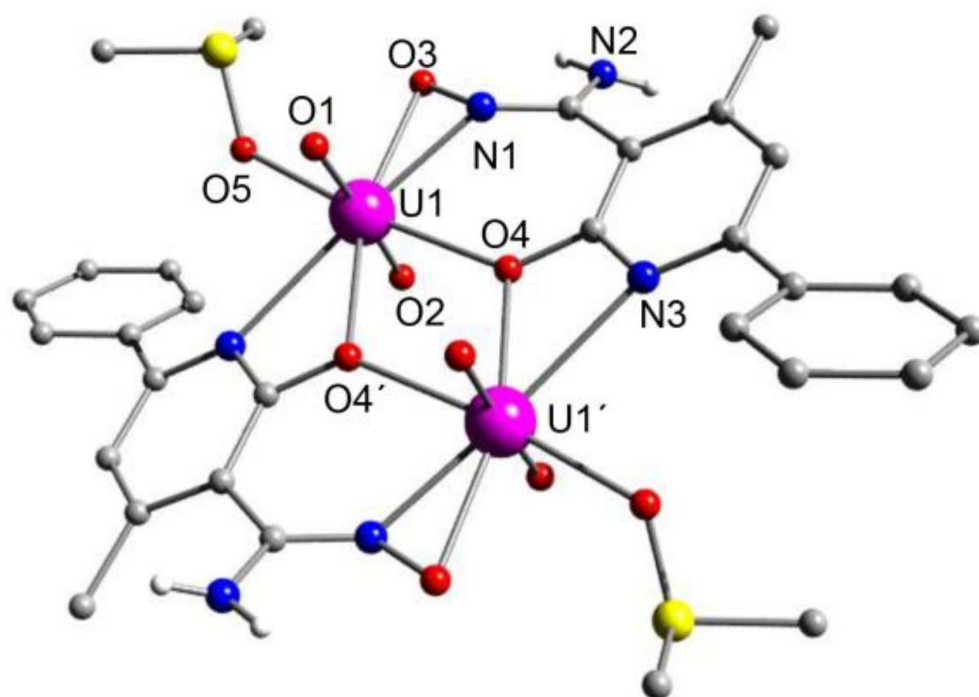
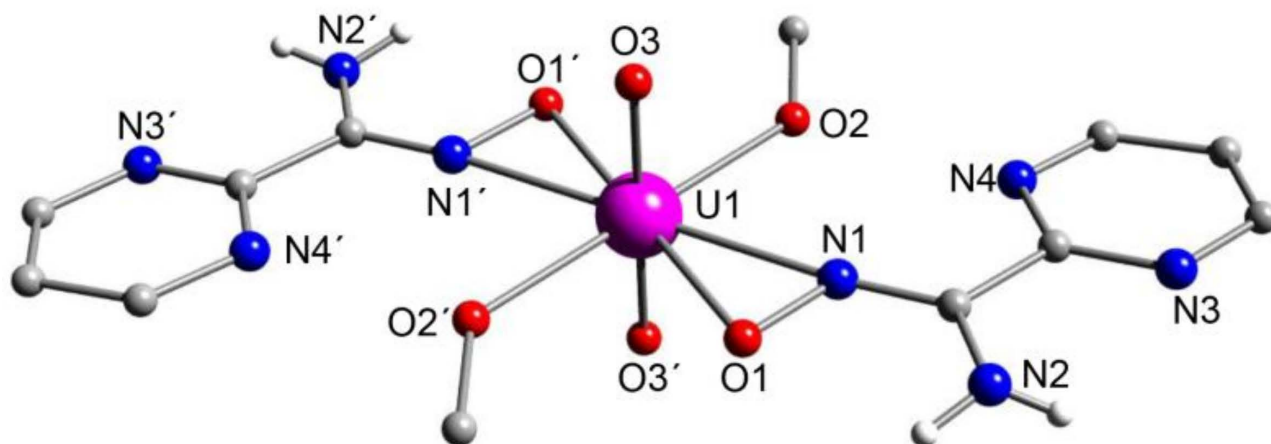


Figure 28. The molecular structure of 19.



**Figure 29.** The molecular structure of 20.

The  $\text{UO}_2(\text{NO}_3)_2 \cdot 6\text{H}_2\text{O}/\text{H}_2\text{pymAO}$  (Figure 7) reaction system in MeOH/MeCN led to the neutral complex  $[\text{UO}_2(\text{HpymAO})_2(\text{MeOH})_2]$  (21) (Figure 30), in which the anionic ligand behaves in the 1.11000 manner (Figure 8), resulting in the formation of two 3-membered ONU chelating rings per uranyl ion ( $\eta^2$  mode of the amidoximato group). The four (4) N atoms of the two pyrimidine rings remain uncoordinated.



**Figure 30.** The molecular structure of 21.

The  $\text{UO}_2(\text{O}_2\text{CMe})_2 \cdot 2\text{H}_2\text{O}/\text{H}_3\text{L5}$  (Figure 7)/ $\text{Et}_3\text{N}$  reaction system in alcohols gave the anionic trinuclear complex  $(\text{Et}_3\text{NH})_2[(\text{UO}_2)_3(\text{O})(\text{O}_2\text{CMe})_3(\text{H}_2\text{L5})_3]$  (22) (Figure 31). The three  $\text{U}^{\text{VI}}$  atoms of the uranyl groups form a  $\mu_3$ -oxo-bridged equilateral triangle, and two neighboring metal ions are further bridged by the O atom of a 2.2010 (Figure 8)  $\text{H}_2\text{L5}^-$  ligand. The amidoxime group of the ligand is neutral.

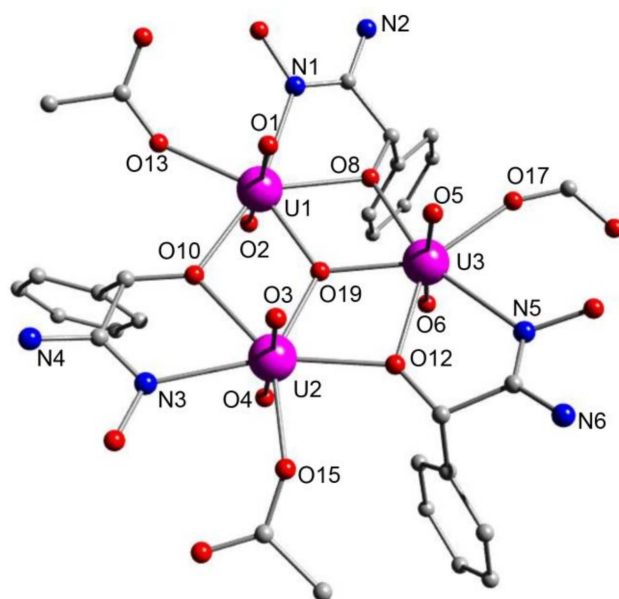


**Figure 31.** The molecular structure of the triangular uranyl dianion that is present in the crystal structure of **22**.

To contribute to the understanding of the  $\{UO_2\}^{2+}/V(IV,V)$  competition in seawater extraction using amidoxime-containing extractants, we performed reactions of H<sub>3</sub>L3, H<sub>3</sub>L4 and H<sub>3</sub>L5 (but also of several diamidoximes), preferably in H<sub>2</sub>O, under aerobic conditions. Working with  $\{V^{IV}O\}^{2+}$  sources, we observed vanadium oxidation in all cases, and no participation of the amidoxime ligands in the inner sphere of V(V). In many reactions, the ligand was transformed into amidinium-type cations, and V(V) was present as a polyoxometalate anionic species. The communication of the ions takes place through H bonds. For example, the reaction between  $[V^{IV}O(acac)_2]$  and H<sub>3</sub>L4 in H<sub>2</sub>O at 80–90 °C leads to the isolation of  $(L6)_6[V^{V}_{10}O_{28}]$  (**III**), where L6<sup>+</sup> is the cation shown in Figure 32.

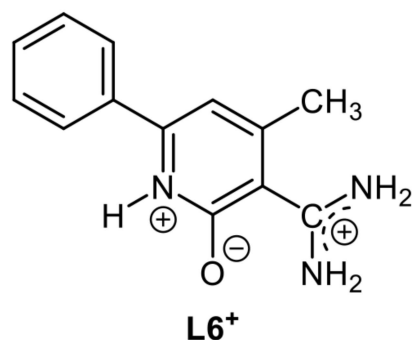


**Figure 32.** The cation that is present in complex  $(L6)_6[V^{V}_{10}O_{28}]$  (**III**); this cation has been derived from the vanadium-assisted/promoted transformation of H<sub>3</sub>L4 (Figure 7).

### 5.9. An overlooked Motif to Uranyl Binding on Poly(Amidoxime) Adsorbents

Understanding the relationship between the amidoxime structural feature on the polymeric sorbent and how this functional group reacts with  $\{UO_2\}^{2+}$  is of great importance to the realization of this metal ion's recovery from the oceans. The structures of functional groups that have been proposed to exist on often used poly(amidoxime) fibers are shown in Figure 6. Using glutardiamidoxime (H<sub>4</sub>B, Figure 17) as a small mimic of the structural motif on sorbent materials, Warner and co-workers discovered that this molecule could undergo in situ cyclization at room temperature in H<sub>2</sub>O/MeOH to 2,6-diimino-piperidin-1-ol (H<sub>3</sub>L7, Figure 33) in the presence of  $UO_2(NO_3)_2 \cdot 6H_2O$  [92]. This was a previously unreported structural motif. The complex isolated was  $[(UO_2)_2(NO_3)_2(H_2L7)_2]$  (**IV**, Figure 34). The two uranyl centers are bridged by the deprotonated O atoms of the two 2.211 H<sub>2</sub>L7<sup>−</sup> ligands

(Figure 33). The cyclic diamino motif can be considered another possible group present on deployed poly(amidoxime) polymers.

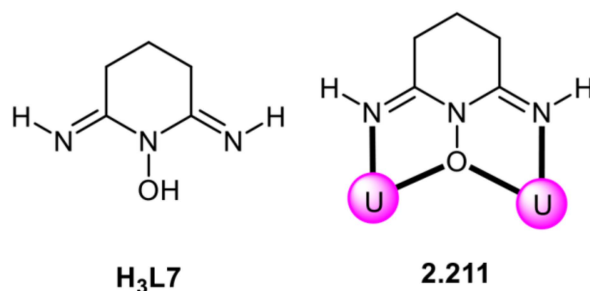


**Figure 33.** The structural formula of 2,6-diimino-piperidin-1-ol and its abbreviation (**left**) and the coordination mode of the singly deprotonated ligand in complex **IV**. The coordination bonds have been drawn with solid lines.

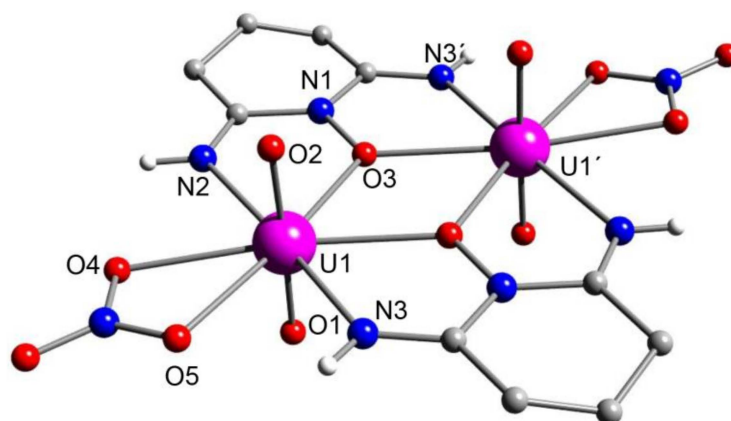


**Figure 34.** The molecular structure of **IV**.

## 6. EXAFS Studies

The extraction of  $\{UO_2\}^{2+}$  from the oceans, which contain ~4.5 billion tons of U, is a promising way to satisfy our increasing demands for nuclear energy. The use of amidoxime-functionalized polymeric adsorbents appears to be the best method for capturing the extremely low concentration of uranium in seawater. Despite intense research for more than 30 years, the exact way in which the amidoxime functionality in aqueous and marine environments interacts with  $\{UO_2\}^{2+}$  is still in dispute. Diffraction methods have been ruled out, while IR and Raman spectroscopic methods (which cannot determine the local coordination environment) are of limited structural information. Coordination chemistry studies in complexes with small amidoxime ligands are also unrealistic, because they cannot represent the actual environment. It is a paradox that most evidence comes from computational studies. The current state of the art is quantitative XAFS analysis combined with theoretical methods. From a plethora of excellent reports, we have chosen to briefly describe two. The first XAFS study of polyamidoxime-bound  $\{UO_2\}^{2+}$  in seawater simulant was reported in 2016 [93], with EXAFS fits suggesting chelation by 2–3 amidoxime functionalities, rather than the tridentate-bound cyclic imidedioxime or  $\eta^2$  motifs that have been generally proposed, mainly based on crystallographic studies. Samples exposed to real seawater also display a feature consistent with a  $Ni^{II}-O^{2-}-\{UO_2\}^{2+}$  subunit in the uranyl coordination sphere, suggesting the in situ formation of a specific binding site or mineralization of uranium on the polymer surface. This motif observed on seawater-contacted polyamidoxime-based polymeric fibers may suggest that a completely different atomic environment is present in seawater-extracted uranyl; this could explain the large reduction in capacity between investigations that take place in simulant and environmental

seawater. It was suggested that  $\{\text{UO}_2\}^{2+}$  sorption in seawater occurs after the in situ formation of an advantageous binding pocket by chelating  $\text{Ni}^{\text{II}}$  [93]. Another excellent combined XAFS and DFT study by Wang's group [94] clarified a years-long debate concerning the exact coordination motif of the amidoxime group with  $\{\text{UO}_2\}^{2+}$ . The study was performed in aqueous solution; it showed that in a highly concentrated amidoxime solution (to model the low  $\text{UO}_2^{2+}$  concentration and the high dose of amidoxime in the local space of the extraction process), the amidoximate group is in the  $\eta^2$  or 1.110 (d in Figure 4) ligation mode and that a tris-amidoximate uranyl species forms (Figure 35), never observed in the solid state by crystallography.

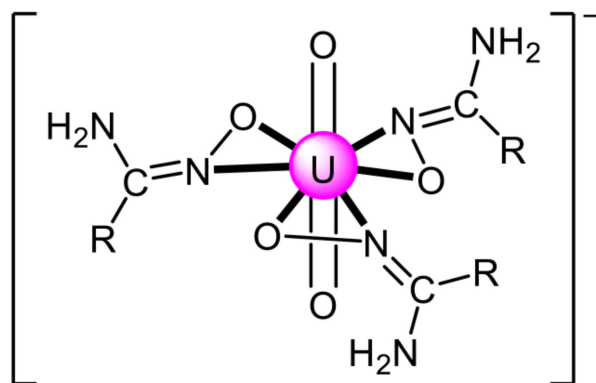


**Figure 35.** The proposed tris-amidoximate anionic uranyl complex that forms in aqueous solution; R is the polymeric backbone. The coordination bonds have been drawn with bold lines.

## 7. Concluding Remarks and Prospects

Previous studies [93,94] might prompt the question as to why a review on the synthesis and structural chemistry of small uranyl-amidoxime complexes is useful. However, these certainly are not accurate representations of the complicated amorphous materials under non-equilibrium conditions in the marine environments. Section 5 demonstrates that the uranyl chemistry with amidoxime ligands, although limited in the number of the to-date structurally characterized complexes, is interesting and diverse. The area of the coordination chemistry of amidoximes has been enriched with new examples and novel ligation modes, e.g., **n** and **o**. From the 15 confirmed coordination modes of the amidoxime group in metal chemistry, illustrated in Figure 4, eight (**a**, **b**, **c**, **d**, **g**, **h**, **n**, **o**) have been crystallographically observed in uranyl chemistry, and some have been proposed to exist under real conditions; thus, X-ray crystallography helps the understanding of the interactions of seawater uranyl ion with the amidoxime. Furthermore, the literature survey, and our results, provide strong evidence that  $\{\text{UO}_2\}^{2+}$ , V(IV) and V(V) interactions proceed through very different coordination modes and geometries, and the V(IV) oxidation state cannot be retained during the reactions.

The conclusions from the structural studies on uranyl-amidoxime complexes should not be exaggerated. It is clear that exposure of polymeric amidoxime-functionalized fibers into environmental seawater and subsequent thorough examination of the extracted materials are key to answering the questions posed at the end of Section 4. From the viewpoint of the structural chemistry of small uranyl-amidoxime complexes, several directions are visible, and our group has been extensively working on them. Some of these include: (a) synthesis of more ligands with two (or even three) amidoxime groups and study of their coordination chemistry with uranyl and vanadium, as well as with other metal ions that are present in seawater ( $\text{Na}^+$ ,  $\text{Mg}^{2+}$ ,  $\text{Ca}^{2+}$ ,  $\text{Fe}^{3+}$ ,  $\text{Ni}^{2+}$ ,  $\text{Cu}^{2+}$ , ...).

(b) Preparation and characterization of heterometallic uranyl-vanadium complexes with amidoxime ligands to elucidate the possible simultaneous coordination of these two metal ions with the amidoxime functionality during the extraction process.

(c) Preparation and study of heterometallic  $\{\text{UO}_2\}^{2+}$ - $\text{Ni}^{\text{II}}$  complexes with amidoxime ligands to provide structural clues on the discovery [93] described above.

(d) Synthesis of anionic uranyl complexes containing three equatorially coordinated  $\eta^2$  amidoximate groups to obtain structural evidence on the exciting proposal raised in reference [94].

(e) X-ray, single-crystal structural studies of the products from  $\text{Ca}_2\text{UO}_2(\text{CO})_3$  [95]/amidoxime ligand reaction systems in order to understand the displacement of carbonates from the naturally occurring form of uranyl in seawater, and confirm the proposed [96] species during the extraction of this ion by polymeric sorbents grafted with amidoxime groups.

(f) Design and synthesis of bifunctional amidoximate-carboxylate ligands and their reactions with  $\{\text{UO}_2\}^{2+}$ , in order to model the reactivity of polymeric sorbents possessing both these groups on the side chains. Such materials exhibit optimal uranyl uptake and great selectivity [97,98], but almost nothing is known about the synergistic effect between the amidoximate and carboxylate functional groups in binding with  $\{\text{UO}_2\}^{2+}$ .

**Author Contributions:** Conceptualization and writing—original draft preparation, S.T.T. and S.P.P.; writing—review and editing, S.T.T., M.I., D.I.T. and S.P.P. All authors have read and agreed to the published version of the manuscript.

**Funding:** This research received no external funding; for the purchase of consumables for our research efforts we would like to thank Theocharis C. Stamatatos and the Chemistry Department of the University of Patras.

**Institutional Review Board Statement:** Not applicable.

**Informed Consent Statement:** Not applicable.

**Data Availability Statement:** Not applicable.

**Conflicts of Interest:** The authors declare no conflict of interest.

## References

1. Liddle, S.T. The Renaissance of Non-Aqueous Uranium Chemistry. *Angew. Chem. Int. Ed.* **2015**, *54*, 8604–8641. [[CrossRef](#)]
2. Bolotin, D.S.; Bokach, N.A.; Kukushkin, V.Y. Coordination chemistry and metal-involving reactions of amidoximes: Relevance to the chemistry of oximes and oxime ligands. *Coord. Chem. Rev.* **2016**, *313*, 62–93. [[CrossRef](#)]
3. Astheimer, L.; Schenk, H.J.; Witte, E.G.; Schwochau, K. Development of Sorbers for the Recovery of Uranium from Seawater. Part 2. The Accumulation of Uranium from Seawater by Resins Containing Amidoxime and Imidoxime Functional Groups. *Sep. Sci. Technol.* **1983**, *18*, 307–339. [[CrossRef](#)]
4. Yue, Y.; Mayes, R.T.; Kim, J.; Fulvio, P.F.; Sun, X.-G.; Tsouris, C.; Chen, J.; Brown, S.; Dai, S. Seawater Uranium Sorbents: Preparation from a Mesoporous Copolymer Initiator by Atom-Transfer Radical Polymerization. *Angew. Chem. Int. Ed.* **2013**, *52*, 13458–13462. [[CrossRef](#)]
5. Das, S.; Oyola, Y.; Mayes, R.T.; Janke, C.J.; Kuo, L.-J.; Gill, G.; Wood, J.R.; Dai, S. Extracting Uranium from Seawater: Promising AF Series Adsorbents. *Ind. Eng. Chem. Res.* **2016**, *55*, 4110–4117. [[CrossRef](#)]
6. Ladshaw, A.P.; Wiechert, A.I.; Das, S.; Yiacoumi, S.; Tsouris, C. Amidoxime Polymers for Uranium Adsorption: Influence of Comonomers and Temperature. *Materials* **2017**, *10*, 1268. [[CrossRef](#)]
7. Dungan, K.; Butler, G.; Livens, F.R.; Warren, L.M. Uranium from seawater-Infinite resource or improbable aspiration? *Prog. Nucl. Energy* **2017**, *99*, 81–85. [[CrossRef](#)]
8. Parker, B.F.; Zhang, Z.; Rao, L.; Arnold, J. An overview and recent progress in the chemistry of uranium extraction from seawater. *Dalton Trans.* **2018**, *47*, 639–644. [[CrossRef](#)]
9. Tang, N.; Liang, J.; Niu, C.; Wang, H.; Luo, Y.; Xing, W.; Ye, S.; Liang, C.; Guo, H.; Guo, J.; et al. Amidoxime-based materials for uranium recovery and removal. *J. Mater. Chem. A* **2020**, *8*, 7588–7625. [[CrossRef](#)]
10. Qin, Z.; Ren, Y.; Shi, S.; Yang, C.; Yu, J.; Wang, S.; Jia, J.; Yu, H.; Wang, X. The enhanced uranyl-amidoxime binding by the electron-donating substituents. *RSC Adv.* **2017**, *7*, 18639–18642. [[CrossRef](#)]
11. Endrizzi, F.; Melchior, A.; Tolazzi, M.; Rao, L. Complexation of uranium(VI) with glutarimidoxime: Thermodynamic and computational studies. *Dalton Trans.* **2015**, *44*, 13835–13844. [[CrossRef](#)] [[PubMed](#)]
12. Sun, X.; Tian, G.; Xu, C.; Rao, L.; Vukovic, S.; Kang, S.O.; Hay, B.P. Quantifying the binding strength of U(VI) with phthalimide-dioxime in comparison with glutarimidedioxime. *Dalton Trans.* **2014**, *43*, 551–557. [[CrossRef](#)] [[PubMed](#)]
13. Abney, C.W.; Liu, S.; Lin, W. Tuning Amidoximate to Enhance Uranyl Binding: A Density Functional Theory Study. *J. Phys. Chem. A* **2013**, *117*, 11558–11565. [[CrossRef](#)] [[PubMed](#)]
14. Yang, C.; Pei, S.; Chen, B.; Ye, L.; Yu, H.; Hu, S. Density functional theory investigations on the binding modes of amidoximes with uranyl ions. *Dalton Trans.* **2016**, *45*, 3120–3129. [[CrossRef](#)]

15. Vukovich, S.; Hay, B.P. De Novo Structure-Based Design of Bis-amidoxime Uranophiles. *Inorg. Chem.* **2013**, *52*, 7805–7810. [[CrossRef](#)]
16. Ladshaw, A.P.; Ivanov, A.S.; Das, S.; Bryantsev, V.S.; Tsouris, C.; Yiacoumi, S. First-Principles Integrated Adsorption Modeling for Selective Capture of Uranium from Seawater by Polyamidoxime Sorbent Materials. *ACS Appl. Mater. Interfaces* **2018**, *10*, 12580–12593. [[CrossRef](#)]
17. Priest, C.; Li, B.; Jiang, D.-E. Uranyl-Glutardiamidoxime Binding from First Principles Molecular Dynamics, Classical Molecular Dynamics, and Free-Energy Simulations. *Inorg. Chem.* **2017**, *56*, 9497–9504. [[CrossRef](#)] [[PubMed](#)]
18. Tsantis, S.T.; Tzimopoulos, D.I.; Holynska, M.; Perlepes, S.P. Oligonuclear Actinoid Complexes with Schiff Bases as Ligands—Older Achievements and Recent Progress. *Int. J. Mol. Sci.* **2020**, *21*, 555. [[CrossRef](#)]
19. Tsantis, S.T.; Lada, Z.G.; Tzimopoulos, D.I.; Bekiari, V.; Psycharis, V.; Raptopoulou, C.P.; Perlepes, S.P. Two different coordination modes of the Schiff base derived from ortho-vanillin and 2-(2-aminomethyl)pyridine in a mononuclear uranyl complex. *Heliyon* **2022**, *8*, e09705. [[CrossRef](#)]
20. Tsantis, S.T.; Bekiari, V.; Raptopoulou, C.P.; Tzimopoulos, D.I.; Psycharis, V.; Perlepes, S.P. Dioxidouranium(VI) complexes with Schiff bases possessing an ONO donor set: Synthetic, structural and spectroscopic studies. *Polyhedron* **2018**, *152*, 172–178. [[CrossRef](#)]
21. Tsantis, S.T.; Danelli, P.; Tzimopoulos, D.I.; Raptopoulou, C.P.; Psycharis, V.; Perlepes, S.P. Pentanuclear Thorium(IV) Coordination Cluster from the Use of Di(2-pyridyl) Ketone. *Inorg. Chem.* **2021**, *60*, 11888–11892. [[CrossRef](#)]
22. Tsantis, S.T.; Lagou-Rekka, A.; Konidaris, K.F.; Raptopoulou, C.P.; Bekiari, V.; Psycharis, V.; Perlepes, S.P. Tetranuclear oxido-bridged thorium(IV) clusters obtained using tridentate Schiff bases. *Dalton Trans.* **2019**, *48*, 15668–15678. [[CrossRef](#)]
23. Tsantis, S.T.; Zagoraiou, E.; Savvidou, A.; Raptopoulou, C.P.; Psycharis, V.; Szyrwił, L.; Holynska, M.; Perlepes, S.P. Binding of oxime group to uranyl ion. *Dalton Trans.* **2016**, *45*, 9307–9319. [[CrossRef](#)]
24. Tsantis, S.T. Chemistry of Uranyl Complexes and Its Relevance to Topical Technological Aspects. Ph.D. Thesis, University of Patras, Patras, Greece, 2020.
25. Iliopoulou, M. Efforts to Structurally Model the Uranyl/Vanadium Competition in Seawater Extraction of Uranium Using Amidoxime Adsorbents. Master's Thesis, University of Patras, Patras, Greece, 2023.
26. Coxall, R.A.; Harris, S.G.; Henderson, D.K.; Parsons, S.; Tasker, P.A.; Winpenny, R.E.P. Inter-ligand reactions: In situ formation of new polydentate ligands. *J. Chem. Soc. Dalton Trans.* **2000**, 2349–2356. [[CrossRef](#)]
27. Abney, C.W.; Mayes, R.T.; Saito, T.; Dai, S. Materials for the Recovery of Uranium from Seawater. *Chem. Rev.* **2017**, *117*, 13935–14013. [[CrossRef](#)]
28. Burns, C.J.; Neu, M.P.; Boukhalfa, H.; Gutowski, K.E.; Bridges, N.J.; Rogers, R.D. The Actinides. In *Comprehensive Coordination Chemistry II*; McCleverty, J.A., Meyer, T.J., Eds.; Elsevier: Amsterdam, The Netherlands, 2003; Volume 3, pp. 189–330.
29. Boreen, M.A.; Arnold, J. The synthesis and versatile reducing power of low-valent uranium complexes. *Dalton Trans.* **2020**, *49*, 15124–15138. [[CrossRef](#)] [[PubMed](#)]
30. Barluzzi, L.; Giblin, S.R.; Mansikkamaki, A.; Layfield, R.A. Identification of Oxidation State +1 in a Molecular Uranium Complex. *J. Am. Chem. Soc.* **2022**, *144*, 18229–18233. [[CrossRef](#)]
31. Bart, S. Bonding with actinides. *Nat. Chem.* **2017**, *9*, 832.
32. Kindra, D.R.; Evans, W.J. Magnetic susceptibility of uranium complexes. *Chem. Rev.* **2014**, *114*, 8865–8882. [[CrossRef](#)] [[PubMed](#)]
33. Raghavan, A.; Anderson, N.H.; Tatebe, C.J.; Stanley, D.A.; Zeller, M.; Bart, S.C. Insight into geometric preferences in uranium(VI) mixed tris(imido) systems. *Chem. Commun.* **2020**, *56*, 11138–11141. [[CrossRef](#)]
34. Andreychuk, N.R.; Vidjayacoumar, B.; Price, J.S.; Kervazo, S.; Peeples, C.A.; Emslie, D.J.H.; Vallet, V.; Gomes, A.S.P.; Real, F.; Schreckenbach, G.; et al. Uranium(IV) alkyl cations: Synthesis, structures, comparison with thorium(IV) analogues, and the influence of arene-coordination on thermal stability and ethylene polymerization activity. *Chem. Sci.* **2022**, *13*, 13748–13763. [[CrossRef](#)] [[PubMed](#)]
35. Knecht, S.; Jensen, H.J.A.; Saue, T. Relativistic quantum chemical calculations show that the uranium molecule U<sub>2</sub> has a quadruple bond. *Nat. Chem.* **2018**, *11*, 40–44. [[CrossRef](#)]
36. Barluzzi, L.; Falcone, M.; Mazzanti, M. Small molecule activation by multimetallic uranium complexes supported by siloxide ligands. *Chem. Commun.* **2019**, *55*, 13031–13047. [[CrossRef](#)]
37. Kaltsoyannis, N. Does Covalency Increase or Decrease across the Actinide Series? Implications for Minor Actinide Partitioning. *Inorg. Chem.* **2013**, *52*, 3407–3413. [[CrossRef](#)] [[PubMed](#)]
38. Hudson, M.J.; Harwood, L.M.; Laventine, D.M.; Lewis, F.W. Use of Soft Heterocyclic N-Donor Ligands to Separate Actinides and Lanthanides. *Inorg. Chem.* **2013**, *52*, 3414–3428. [[CrossRef](#)] [[PubMed](#)]
39. King, D.M.; Cleaves, P.A.; Wooles, A.J.; Gardner, B.M.; Chilton, N.F.; Tuna, F.; Lewis, W.; McInnes, E.J.L.; Liddle, S.T. Molecular and electronic structure of terminal and alkali metal-capped uranium(V) nitride complexes. *Nat. Commun.* **2016**, *7*, 13773. [[CrossRef](#)]
40. Meihaus, K.R.; Long, J.R. Actinide-based single-molecule magnets. *Dalton Trans.* **2015**, *44*, 2517–2528. [[CrossRef](#)]
41. Mills, D.P.; Moro, F.; McMaster, J.; van Slageren, J.; Lewis, W.; Blake, A.J.; Liddle, S.T. A delocalized arene-bridged diuranium single-molecule magnet. *Nat. Chem.* **2011**, *3*, 454–460. [[CrossRef](#)]
42. Dey, S.; Velmurugan, G.; Rajaraman, G. How important is the coordinating atom in controlling magnetic anisotropy in uranium(III) single-ion magnets? A theoretical perspective. *Dalton Trans.* **2019**, *48*, 8976–8988. [[CrossRef](#)]

43. Fortier, S.; Hayton, T.W. Oxo ligand functionalization in the uranyl ion ( $\text{UO}_2^{2+}$ ). *Coord. Chem. Rev.* **2010**, *254*, 197–214. [[CrossRef](#)]
44. Cowie, B.E.; Purkis, J.M.; Austin, J.; Love, J.B.; Arnold, P.L. Thermal and Photochemical Reduction and Functionalization Chemistry of the Uranyl Dication,  $[\text{U}^{\text{VI}}\text{O}_2]^{2+}$ . *Chem. Rev.* **2019**, *119*, 10595–10637. [[CrossRef](#)] [[PubMed](#)]
45. Ai, J.; Chen, F.-Y.; Gao, C.-Y.; Tian, H.-R.; Pan, Q.-J.; Sun, Z.-M. Porous anionic uranyl-organic networks for highly efficient  $\text{Cs}^+$  adsorption and investigation of the mechanism. *Inorg. Chem.* **2018**, *57*, 4419–4426. [[CrossRef](#)] [[PubMed](#)]
46. Rudkevich, D.M.; Verboom, W.; Brzozka, A.; Palys, M.J.; Stauthamer, W.P.R.V.; van Hummel, G.J.; Franken, S.M.; Harkema, S.; Engbersen, J.F.J.; Reinhoudt, D.N. Functionalized  $\text{UO}_2$  salenes: Neutral receptor for anions. *J. Am. Chem. Soc.* **1994**, *116*, 4341–4351. [[CrossRef](#)]
47. Odoh, S.O.; Bondarevsky, G.D.; Karpus, J.; Cui, Q.; He, C.; Spezia, R.; Gagliardi, L.  $\text{UO}_2^{2+}$  uptake by proteins: Understanding the binding features of the super uranyl binding protein and design of a protein with higher affinity. *J. Am. Chem. Soc.* **2014**, *136*, 17484–17494. [[CrossRef](#)]
48. Xu, M.; Eckard, P.; Burns, P.C. Organic Functionalization of Uranyl Peroxide Clusters to Impact Solubility. *Inorg. Chem.* **2020**, *59*, 9881–9888. [[CrossRef](#)] [[PubMed](#)]
49. Gutowski, K.E.; Cocalia, V.A.; Griffin, S.T.; Bridges, N.J.; Dixon, D.A.; Rogers, R.D. Interactions of 1-methylimidazole with  $\text{UO}_2(\text{CH}_3\text{CO}_2)_2$  and  $\text{UO}_2(\text{NO}_3)_2$ : Structural, spectroscopic, and theoretical evidence for imidazole binding to the uranyl ion. *J. Am. Chem. Soc.* **2007**, *129*, 526–536. [[CrossRef](#)]
50. Tshipis, A.C. cis- and trans-Ligand Effects of the Inverse trans-Influence in  $[\text{U}^{\text{VI}}(\text{O})(\text{L})\text{Cl}_4]^{0/-}$  (L=Unidentate Ligand) Complexes. *Inorg. Chem.* **2020**, *59*, 8946–8959. [[CrossRef](#)]
51. Harrowfield, J.; Thuery, P. Uranyl Ion Complexes of Polycarboxylates: Steps towards Isolated Photoactive Cavities. *Chemistry* **2020**, *2*, 63–79. [[CrossRef](#)]
52. Costisor, O.; Linert, W. 4f and 5f metal ion directed Schiff condensation. *Rev. Inorg. Chem.* **2004**, *24*, 61–95. [[CrossRef](#)]
53. Van Axel Castelli, V.; Cort Dalla, A.; Mandolini, L. Supramolecular catalysis of 1,4-thiol addition by salophen-uranyl complexes. *J. Am. Chem. Soc.* **1998**, *120*, 12688–12689. [[CrossRef](#)]
54. Hawkins, C.A.; Bustillos, C.G.; Copping, R.; Scott, B.L.; May, I.; Nilsson, M. Challenging conventional f-element separation chemistry-reversing uranyl(VI)/lanthanide(III) solvent extraction selectivity. *Chem. Commun.* **2014**, *50*, 8670–8673. [[CrossRef](#)]
55. Weng, Z.; Zhang, Z.-h.; Olds, T.; Sterniczuk, M.; Burns, P.C. Copper(I) and Copper(II) Uranyl Heterometallic Hybrid Materials. *Inorg. Chem.* **2014**, *53*, 7993–7998. [[CrossRef](#)]
56. Xie, J.; Wang, Y.; Silver, M.A.; Liu, W.; Duan, T.; Yin, X.; Chen, L.; Diwu, J.; Chai, Z.; Wang, S. Tunable 4f/5f Bimodal Emission in Europium-Incorporated Uranyl Coordination Polymers. *Inorg. Chem.* **2018**, *57*, 575–582. [[CrossRef](#)]
57. Behera, N.; Sethi, S. Unprecedented Catalytic Behavior of Uranyl(VI) Compounds in Chemical Reactions. *Eur. J. Inorg. Chem.* **2021**, *2021*, 95–111. [[CrossRef](#)]
58. Sahyoun, T.; Arrault, A.; Schneider, R. Amidoximes and Oximes: Synthesis, Structure, and Their Key Role as NO Donors. *Molecules* **2019**, *24*, 2470. [[CrossRef](#)]
59. Efthymiou, C.G.; Cunha-Silva, L.; Perlepes, S.P.; Brechin, E.K.; Inglis, R.; Evangelisti, M.; Papatriantafyllopoulou, C. In search of molecules displaying ferromagnetic exchange: Multiple-decker  $\text{Ni}_{12}$  and  $\text{Ni}_{16}$  complexes from the use of pyridine-2-amidoxime. *Dalton Trans.* **2016**, *45*, 17409–17419. [[CrossRef](#)] [[PubMed](#)]
60. Novikov, A.S.; Bolotin, D.S. Tautomerism of amidoximes and other oximes species. *J. Phys. Org. Chem.* **2018**, *31*, e3772. [[CrossRef](#)]
61. Tavakol, H.; Arshadi, S. Theoretical investigation of tautomerism in N-hydroxy amidines. *J. Mol. Model.* **2009**, *15*, 807–816. [[CrossRef](#)] [[PubMed](#)]
62. Duros, V.; Sartzi, H.; Teat, S.J.; Sanakis, Y.; Roubeau, O.; Perlepes, S.P.  $\text{Tris}\{2,4\text{-bis}(2\text{-pyridyl})\text{-}1,3,5\text{-triazapentanedienato}\}\text{manganese(III)}$ , a complex derived from a unique metal ion-assisted transformation of pyridine-2-amidoxime. *Inorg. Chem. Commun.* **2014**, *50*, 117–121. [[CrossRef](#)]
63. Tsouris, C. Fuel from seawater. *Nat. Energy* **2017**, *2*, 17022. [[CrossRef](#)]
64. Das, S.; Oyola, Y.; Mayes, R.T.; Janke, C.J.; Kuo, L.-J.; Gill, G.; Wood, J.R.; Dai, S. Extracting Uranium from Seawater: Promising AI Series Adsorbents. *Ind. Eng. Chem. Res.* **2016**, *55*, 4103–4109. [[CrossRef](#)]
65. Gill, G.A.; Kuo, L.-J.; Janke, C.J.; Park, J.; Jetters, R.T.; Bonheyo, G.T.; Pan, H.-B.; Wai, C.; Khangaonkar, T.; Bianucci, L.; et al. The Uranium from Seawater Program at the Pacific Northwest National Laboratory: Overview of Marine Testing, Adsorbent Characterization, Adsorbent Durability, Adsorbent Toxicity, and Deployment Studies. *Ind. Eng. Chem. Res.* **2016**, *55*, 4264–4277. [[CrossRef](#)]
66. Davies, R.V.; Kennedy, J.; McIlroy, R.W.; Spence, R.; Hill, K.M. Extraction of Uranium from Sea Water. *Nature* **1964**, *203*, 1110–1115. [[CrossRef](#)]
67. Schenk, H.J.; Astheimer, L.; Witte, E.G.; Schwochau, K. Development of Sorbers for the Recovery of Uranium from Seawater. 1. Assessment of Key Parameters and Screening Studies of Sorber Materials. *Sep. Sci. Technol.* **1982**, *17*, 1293–1308. [[CrossRef](#)]
68. Yue, Y.; Mayes, R.T.; Gill, G.; Kuo, L.-J.; Wood, J.; Binder, A.; Brown, S.; Dai, S. Macroporous monoliths for trace metal extraction from seawater. *RSC Adv.* **2015**, *5*, 50005–50010. [[CrossRef](#)]
69. Hu, J.; Ma, H.; Xing, Z.; Liu, X.; Xu, L.; Li, R.; Lin, C.; Wang, M.; Li, J.; Wu, G. Preparation of Amidoximated Ultrahigh Molecular Weight Polyethylene Fiber by Radiation Grafting and Uranium Adsorption Test. *Ind. Eng. Chem. Res.* **2016**, *55*, 4118–4124. [[CrossRef](#)]

70. Mehio, N.; Lashley, M.A.; Nugent, J.W.; Tucker, L.; Correia, B.; Do-Thanh, C.-L.; Dai, S.; Hancock, R.D.; Bryantsev, V.S. Acidity of the Amidoxime Functional Group in Aqueous Solution: A Combined Experimental and Computational Study. *J. Phys. Chem. B* **2015**, *119*, 3567–3576. [[CrossRef](#)]
71. Lashley, M.; Mehio, N.; Nugent, J.W.; Holguin, E.; Do-Thanh, C.-L.; Bryantsev, V.S.; Dai, S.; Hancock, R.D. Amidoximes as ligand functionalities for braided polymeric materials for the recovery of uranium from seawater. *Polyhedron* **2016**, *109*, 81–91. [[CrossRef](#)]
72. Aguila, B.; Sun, Q.; Cassady, H.; Abney, C.W.; Li, B.; Ma, S. Design Strategies to Enhance Amidoxime Chelators for Uranium Recovery. *ACS Appl. Mater. Interfaces* **2019**, *11*, 30919–30926. [[CrossRef](#)]
73. Wu, Y.; Xie, Y.; Liu, X.; Li, Y.; Wang, J.; Chen, Z.; Yang, H.; Hu, B.; Chen, C.; Tang, Z.; et al. Functional nanomaterials for selective uranium recovery from seawater: Material design, extraction properties and mechanisms. *Coord. Chem. Rev.* **2023**, *483*, 215097. [[CrossRef](#)]
74. Liu, C.; Hsu, P.-C.; Xie, J.; Zhao, J.; Wu, T.; Wang, H.; Liu, W.; Zhang, J.; Chu, S.; Cui, L. A half-wave rectified alternating current electrochemical method for uranium extraction from seawater. *Nat. Energy* **2017**, *2*, 17007. [[CrossRef](#)]
75. Witte, E.G.; Schowochau, K.S.; Henkel, G.; Krebs, B. Uranyl Complexes of Acetamidoxime and Benzamidoxime. Preparation, Characterization, and Crystal Structure. *Inorg. Chim. Acta* **1984**, *94*, 323–331. [[CrossRef](#)]
76. Kravchuk, D.V.; Diaz, A.B.; Carolan, M.E.; Mpundu, E.A.; Cwiertny, D.M.; Forbes, T.Z. Uranyl Speciation on the Surface of the Amidoximated Polyacrylonitrile Mats. *Inorg. Chem.* **2020**, *59*, 8134–8145. [[CrossRef](#)]
77. Vukovic, S.; Watson, L.A.; Kang, S.O.; Custelcean, R.; Hay, B.P. How Amidoximate Binds the Uranyl Cation. *Inorg. Chem.* **2012**, *51*, 3855–3859. [[CrossRef](#)] [[PubMed](#)]
78. Barber, P.S.; Kelley, S.P.; Rogers, R.D. Highly selective extraction of the uranyl ion with hydrophobic amidoxime-functionalized ionic liquids via  $\eta^2$  coordination. *RSC Adv.* **2012**, *2*, 8526–8530. [[CrossRef](#)]
79. Tian, G.; Teat, S.J.; Zhang, Z.; Rao, L. Sequestering uranium from seawater: Binding strength and modes of uranyl complexes with glutarimidedioxime. *Dalton Trans.* **2012**, *41*, 11579–11586. [[CrossRef](#)]
80. Bernstein, K.J.; Do-Thanh, C.-L.; Penchoff, D.A.; Cramer, S.A.; Murdock, C.R.; Lu, Z.; Harrison, R.J.; Camden, J.P.; Jenkins, D.M. The synthesis and spectroscopic characterization of an aromatic uranium amidoxime complex. *Inorg. Chim. Acta* **2014**, *421*, 374–379. [[CrossRef](#)]
81. Kelley, S.P.; Barber, P.S.; Mullins, P.H.K.; Rogers, R.D. Structural clues to  $\text{UO}_2^{2+}/\text{VO}_2^+$  competition in seawater using amidoxime-based extractants. *Chem. Commun.* **2014**, *50*, 12504–12507. [[CrossRef](#)]
82. Sun, Q.; Aguila, B.; Perman, J.; Ivanov, A.S.; Bryantsev, V.S.; Earl, L.D.; Abney, C.W.; Wojtas, L.; Ma, S. Bio-inspired nano-traps for uranium extraction from seawater and recovery from nuclear waste. *Nat. Commun.* **2018**, *9*, 1644. [[CrossRef](#)]
83. Mishra, M.K.; Patil, V.; Kelley, S.P.; Rogers, R.D. A Uranyl Metal Organic Framework Arising from the Coordination of a Partially Hydrolyzed Tetrauranyl Mode with the Tautomericly Diverse 1,4-(diamidoximyl)benzene Ligand. *Crystal Growth Des.* **2019**, *19*, 5466–5470. [[CrossRef](#)]
84. Decato, D.A.; Berryman, O.B. Structural and computational characterization of a bridging zwitterionic-amidoxime uranyl complex. *Org. Chem. Front.* **2019**, *6*, 1038–1043. [[CrossRef](#)]
85. Parker, B.F.; Hohloch, S.; Pankhurst, J.R.; Zhang, Z.; Love, J.B.; Arnold, J.; Rao, L. Interactions of vanadium ligands: Redox activity. *Dalton Trans.* **2018**, *47*, 5695–5702. [[CrossRef](#)] [[PubMed](#)]
86. Tian, G.; Teat, S.J.; Rao, L. Thermodynamic studies of U(VI) complexation with glutardiamidoxime for sequestration of uranium from seawater. *Dalton Trans.* **2013**, *42*, 5690–5696. [[CrossRef](#)] [[PubMed](#)]
87. Ivanov, A.S.; Leggett, C.J.; Parker, B.F.; Zhang, Z.; Arnold, J.; Dai, S.; Abney, C.W.; Bryantsev, V.S.; Rao, L. Origin of the unusually strong and selective binding of vanadium by polyamidoximes in seawater. *Nat. Commun.* **2017**, *8*, 1560. [[CrossRef](#)]
88. Mehio, N.; Ivanov, A.S.; Ladshaw, A.P.; Dai, S.; Bryantsev, V.S. Theoretical Study of Oxovanadium(IV) complexation with formamidoximate: Implications for the Design of Uranyl-Selective Adsorbents. *Ind. Eng. Chem. Res.* **2016**, *55*, 4231–4240. [[CrossRef](#)]
89. Mehio, N.; Johnson, J.C.; Dai, S.; Bryantsev, V.S. Theoretical study of the coordination behavior of formate and formamidoximate with dioxovanadium(V) cation: Implications for selectivity towards uranyl. *Phys. Chem. Chem. Phys.* **2015**, *17*, 31715–31726. [[CrossRef](#)] [[PubMed](#)]
90. Parker, B.F.; Zhang, Z.; Leggett, C.J.; Arnold, J.; Rao, L. Kinetics of complexation of V(V), U(VI) and Fe(III) with glutarimidedioxime: Studies by stopped-flow and conventional adsorption spectroscopy. *Dalton Trans.* **2017**, *46*, 11084–11096. [[CrossRef](#)]
91. Ivanov, A.S.; Bryantsev, V.S. Assessing ligand selectivity for uranium over vanadium ions to aid in the discovery of superior adsorbents for extraction of  $\text{UO}_2^{2+}$  from seawater. *Dalton Trans.* **2016**, *45*, 10744–10751. [[CrossRef](#)]
92. Kennedy, Z.C.; Cardenas, A.J.P.; Corbey, J.F.; Warner, M.G. 2,6-Diiminopiperidin-1-ol: An overlooked motif relevant to uranyl and transition metal binding on poly(amidoxime) adsorbents. *Chem. Commun.* **2016**, *52*, 8802–8805. [[CrossRef](#)]
93. Abney, C.W.; Mayes, R.T.; Piechowicz, M.; Lin, Z.; Bryantsev, V.S.; Veith, G.M.; Dai, S.; Lin, W. XAFS investigation of polyamidoxime-bound uranyl contests the paradigm from small molecule studies. *Energy Environ. Sci.* **2016**, *9*, 448–453. [[CrossRef](#)]
94. Zhang, L.; Qie, M.; Su, J.; Zhang, S.; Zhou, J.; Li, J.; Wang, Y.; Yang, S.; Wang, S.; Li, J.; et al. Tris-amidoximate uranyl via  $\eta^2$  binding mode coordinated in aqueous solution shown by X-ray absorption spectroscopy and density functional theory methods. *J. Synchrotron Rad.* **2018**, *25*, 514–522. [[CrossRef](#)] [[PubMed](#)]

95. Endrizzi, F.; Rao, L. Chemical Speciation of Uranium(VI) in Marine Environments: Complexation of Calcium and Magnesium Ions with  $[(\text{UO}_2)(\text{CO}_3)_3]^{4-}$  and the Effect on the Extraction of Uranium from Seawater. *Chem. Eur. J.* **2014**, *20*, 14499–14506. [[CrossRef](#)] [[PubMed](#)]
96. Li, B.; Priest, C.; Jiang, D.-E. Displacement of carbonates in  $\text{Ca}_2\text{UO}_2(\text{CO}_3)_3$  by amidoxime-based ligands from free-energy simulations. *Dalton Trans.* **2018**, *47*, 1604–1613. [[CrossRef](#)]
97. Priest, C.; Li, B.; Jiang, D.-E. Understanding the Binding of a Bifunctional Amidoximate-Carboxylate Ligand with Uranyl in Seawater. *J. Phys. Chem. B* **2018**, *122*, 12060–12066. [[CrossRef](#)] [[PubMed](#)]
98. Wang, C.-Z.; Lan, J.-H.; Wu, Q.-Y.; Luo, Q.; Zhao, Y.-L.; Wang, X.-K.; Chai, Z.-F.; Shi, W.-Q. Theoretical Insights on the Interaction of Uranium with Amidoxime and Carboxyl Groups. *Inorg. Chem.* **2014**, *53*, 9466–9476. [[CrossRef](#)]

**Disclaimer/Publisher's Note:** The statements, opinions and data contained in all publications are solely those of the individual author(s) and contributor(s) and not of MDPI and/or the editor(s). MDPI and/or the editor(s) disclaim responsibility for any injury to people or property resulting from any ideas, methods, instructions or products referred to in the content.